Differential neuropeptide modulation of premotor and motor neurons in the lobster cardiac ganglion

Emily R. Oleisky[1], Meredith E. Stanhope[1], J. Joe Hull[2], Andrew E. Christie[3], Patsy S. Dickinson[1]*

[1]Department of Biology, Bowdoin College, 6500 College Station, Brunswick, ME 04011, USA.

[2]Pest Management and Biocontrol Research Unit, US Arid Land Agricultural Research Center, USDA Agricultural Research Services, Maricopa, AZ 85138, USA.

[3]Békésy Laboratory of Neurobiology, Pacific Biosciences Research Center, School of Ocean and Earth Science and Technology, University of Hawaii at Manoa, 1993 East-West Road, Honolulu, HI 96822, USA.

Abbreviated Title (for running head): Neuropeptide modulation of neurons in the cardiac ganglion

***Corresponding Author:** Patsy S. Dickinson (pdickins@bowdoin.edu)
Department of Biology, Bowdoin College, 6500 College Station, Brunswick, ME 04011, USA. Phone (207) 725-3581

NEW & NOTEWORTHY

Premotor and motor neurons of the *Homarus americanus* cardiac ganglion (CG) are normally electrically and chemically coupled, and generate rhythmic bursting that drives cardiac contractions; we show that they can establish independent bursting patterns when physically decoupled by a ligature. The neuropeptide myosuppressin modulates different aspects of the bursting pattern in these neuron types to determine the overall modulation of the intact CG. Differential distribution of myosuppressin receptors may underlie the observed responses to myosuppressin.

KEYWORDS: central pattern generator; cardiac ganglion; myosuppressin; neuropeptide; *Homarus americanus*

ABSTRACT

The American lobster, *Homarus americanus*, cardiac neuromuscular system is controlled by the cardiac ganglion (CG), a central pattern generator consisting of four premotor and five motor neurons. Here, we show that the premotor and motor neurons can establish independent bursting patterns when decoupled by a physical ligature. We also show that mRNA encoding myosuppressin, a cardioactive neuropeptide, is produced within the CG. We thus asked whether myosuppressin modulates the decoupled premotor and motor neurons, and, if so, how this modulation might underlie the role(s) that these neurons play in myosuppressin's effects on ganglionic output. Although myosuppressin exerted dose-dependent effects on burst frequency and duration in both premotor and motor neurons in the intact CG, its effects on the ligatured ganglion were more complex, with different effects and thresholds on the two types of neurons. These data suggest that the motor neurons are more important in determining the changes in frequency of the CG elicited by low concentrations of myosuppressin, whereas the premotor neurons have a greater impact on changes elicited in burst duration. A single putative myosuppressin receptor (MSR-I) was previously described from the *Homarus* nervous system. We identified four additional putative MSRs (MSR-II-V) and investigated their individual distributions in the CG premotor and motor neurons using RT-PCR. Transcripts for only three receptors (MSR-II-IV) were amplified from the CG. Potential differential distributions of the receptors were observed between the premotor and motor neurons; these differences may contribute to the distinct physiological responses of the two neuron types to myosuppressin.

INTRODUCTION

Flexibility in neuronal output underlies the ability of pattern generating networks to elicit a wide array of rhythmic movements (e.g., breathing, locomotion); such flexibility is frequently achieved by the action of neuromodulators (Delcomyn 1980; Marder and Calabrese 1996). Both circulating hormones and locally released neuromodulators have been shown to act on neural networks to elicit the physiological changes that lead to changes in behavioral output, although they generally do so at different concentrations (Dickinson et al. 2019a; Dickinson et al. 2015; Messinger et al. 2005). While a wide range of molecules can serve as neuromodulators, peptides comprise the largest and most diverse group (Brezina 2010; Briggman and Kristan 2008; Christie et al. 2010a).

The decapod crustacean cardiac neuromuscular system is a model for understanding the modulatory control of rhythmic motor behavior (Cooke 2002). This simple central pattern generator (CPG)-effector system is composed of the cardiac ganglion (CG), i.e., the CPG, and the heart musculature, i.e., the effector system. In the American lobster, *Homarus americanus*, the CG consists of nine neurons (Figure 1A): four small, posteriorly positioned premotor neurons (alternatively termed the small cells or pacemaker neurons) and five large, anteriorly located motor neurons (also referred to as the large cells). These two types of neurons are both electrically and chemically coupled and exhibit spontaneous in-phase bursting activity (Cooke 2002; Williams et al. 2013). The premotor neurons have classically been viewed as driving rhythmic activity in the CG by synapsing onto and promoting burst activity in motor cells (Hartline 1967). The motor neurons send feedback to the premotor neurons, and endogenous driver potentials contribute to the regulation of burst frequency (Berlind 1989; Mayeri 1973). The collective actions of the two neuron types produce bursts of action potentials that drive heart contractions (Cooke 2002). We report here that the premotor and motor neurons of the lobster CG can establish independent bursting patterns when physically decoupled by a ligature. Since peptides have been shown to alter the crustacean CPG bursting behavior at both the level of the isolated ganglion and the periphery of the cardiac neuromuscular system (Dickinson et al. 2007; Fort et al. 2007a; Fort et al. 2007b; Stevens et al. 2009), we asked

whether the separated neuronal types were independently modulated, and if so, what roles each neuron type might play in the modulation of the pattern as a whole.

Myosuppressin (pQDLDHVFLRFamide), a highly conserved decapod neuropeptide (Stemmler et al. 2007), has been shown to act at multiple sites within the cardiac neuromuscular system of the lobster. In the whole heart, myosuppressin (10^{-7} M) decreases heart contraction frequency and causes an initial decrease in contraction amplitude followed by a large increase in amplitude. In the isolated CG, myosuppressin elicits a decrease in burst frequency and an increase in burst duration, with the threshold for effects at ~10^{-7} M. When motor input was removed from the heart and an electrode was used to deliver an electrical stimulus mimicking the CG bursting pattern, amplitudes of cardiac contractions increased in the presence of 10^{-7} M myosuppressin, suggesting that myosuppressin acts at the neuromuscular junction or muscle as well as in the CG itself to elicit whole heart responses (Stevens et al. 2009).

In this study, we investigated whether myosuppressin was capable of independently modulating the premotor and motor neurons of the CG, and, if so, how such modulation might underlie the role of these neurons in the coordinated motor pattern. Because many of the effects of myosuppressin recorded previously and in the present study are evident only at concentrations that are consistent with local rather than hormonal release (i.e., 10^{-6} M rather than 10^{-7} to 10^{-9} M; Dickinson et al. 2019a; Dickinson et al. 2015; Messinger et al. 2005), we asked whether myosuppressin is likely to be present within the neurons of the CG. In support of this, we found putative myosuppressin-encoding transcripts expressed in the neurons of the CG. Finally, to elucidate mechanisms that may underlie the differential effects on the two neuronal types in the CG, we asked whether the CG expressed more than one myosuppressin receptor, and if so, whether they are differentially distributed in the premotor and motor neurons. One putative myosuppressin receptor had previously been identified from a *H. americanus* mixed tissue transcriptome (Christie et al. 2015). In the present study, transcriptomic analyses revealed four additional putative myosuppressin receptors in *H. americanus* neural tissues (MSR-II-V). Profiling of isolated premotor and motor neuron regions of the CG revealed expression of

hyphenate?

three of the MSRs (MSR-II, MSR-III, and MSR-IV) in the ganglion. Moreover, at least some of these receptors appear to be differentially expressed in the two neuron types, suggesting that differential receptor distribution may underlie, at least in part, the distinct physiological responses of the premotor and motor neurons to myosuppressin.

MATERIALS AND METHODS

Animals

Adult (~500 g) *H. americanus* were purchased from local seafood suppliers (Brunswick, Maine, USA); the individuals used included males and females and represented all stages of the molt cycle. Lobsters were housed in re-circulating natural seawater aquaria and were maintained on a 12-hr/12-hr light/dark cycle at 10-12°C. The lobsters were fed a weekly diet of chopped shrimp or squid.

Individual lobsters were anesthetized by packing in ice for ~30 min prior to isolation of the heart from the cephalothoracic carapace via manual microdissection in chilled (8–10°C) physiological saline (composition in $mmol^{-1}$: 479.12 NaCl, 12.74 KCl, 13.67 $CaCl_2$, 20.00 $MgSO_4$, 3.91 Na_2SO_4, 11.45 Trizma base and 4.82, maleic acid; pH: 7.45; Dickinson et al. 2018). To isolate the CG, the heart was opened along the ventral axis and the main trunk of the ganglion, along with lengths of the anterolateral nerves, was dissected from the surrounding musculature (Figure 1A).

Physiology

Separation of the premotor and motor neurons

A single fiber taken from a length of 0.1 mm 6-0 suture silk was used as a ligature to tie a slack knot around the trunk of the CG just anterior to motor neuron 4 (Figure 1A). Premotor neuron spike initiation zones extend from the most distal premotor neuron cell body to the soma of motor neuron 4 (Hartline 1967). This ligature placement ensured that the premotor neuron spike initiation zones were left intact, but were active only in the portion of the CG posterior to the ligature once it was tightened (Figure 1B). Successful

placement of the ligature was confirmed when only premotor neuron spikes were recorded on the trunk and only motor neuron spikes were recorded on the anterolateral nerves after the ligature was tightened. Because cutting the ganglion evokes injury discharges in recordings of both premotor and motor neurons in an intact ganglion, we cut the CG at the end of the experiment either just anterior or just posterior to the ligature; we then observed the bursting pattern of the cells on the non-disrupted side of the ligature to verify the ability of the ligature method to separate the cell types.

Recordings

Petroleum jelly wells were built around small portions of the anterolateral nerves to monitor motor neuron output and around the trunk of the ganglion to monitor premotor neuron output (Figure 1A; Williams et al. 2013). Bipolar stainless steel electrodes were used for extracellular recordings, with one electrode in the well and the other nearby in the bath. Neuronal output was amplified with a 1700 A-M Systems Differential AC amplifier (Sequim, WA, USA) and a 440 Brownlee Precision amplifier (Brownlee Instruments, San Jose, CA, USA), digitized with a CED Micro 1401 digitizer and recorded using Spike2 version 7.17 (Cambridge Electronic Design, Cambridge, UX), with a sampling rate of 10kHz.

add space between # and unit

Temperature was maintained throughout recordings between 10-12°C via an in-line Peltier temperature regulator (CL-100 bipolar temperature controller and SC-20 solution heater/cooler; Warner Instruments, Hamden, CT, USA) with a temperature probe (Warner Instruments, Hamden, CT, USA). Physiological saline was superfused at a flow rate of ~5 ml min^{-1} across the ganglion using a Rabbit peristaltic pump (Gilson, Middleton, WI, USA). Myosuppressin (pQDLDHVFLRFamide), custom synthesized by GenScript Corporation (Piscataway, NJ, USA), was introduced into the bath with the CG via the perfusion pump. Due to the relatively low aqueous solubility of myosuppressin, the peptide was dissolved in DMSO, and then diluted in deionized water to make 10^{-3} M stock solutions containing 15% DMSO (Stevens et al. 2009). When diluted, the concentration of DMSO was at most 0.015%, which did not alter CG bursting patterns when superfused over the ganglion. Solutions were stored in small aliquots at -25°C, and diluted in saline to the appropriate concentration directly preceding use.

After superperfusion of the intact CG with myosuppressin (10^{-7} or 10^{-6} M, 10 min peptide application) and a 45 min saline wash, the ligature was tightened to physically decouple the premotor and motor neurons, in an attempt to eliminate chemical and electrical communication between neuron types. After a return of bursting activity in isolated neuron types, the ligatured CG was again superfused with myosuppressin at 10^{-7} or 10^{-6} M.

Data Analysis

Physiological recordings were analyzed using functions built into Spike2, version 7.17, and scripts previously generated by the STG Laboratory at NJIT Rutgers (http://stg.rutgers.edu/Resources.html). Data were averaged over ten bursts, with control values taken shortly before the addition of the peptide to the bath and peptide values taken at the peak of the peptide effect, near the end of the 10 min peptide application. A burst was defined as a trail of at least five action potentials ("spikes") occurring at a frequency of at least 100Hz. Burst duration was quantified separately for the premotor and motor neurons in both intact and ligatured CG preparations as the duration from the first to the last spike in a given burst. Interburst interval was the length of time between successive bursts. Burst frequencies recorded in the premotor and motor neurons of the intact CG were identical, as premotor and motor neurons are coupled and burst in phase with one another (Williams et al. 2013). In ligatured CG preparations, the burst frequencies of the premotor and motor neurons were quantified separately, as the neurons had been physically decoupled. A trail of low frequency tonic or irregular spikes ("leading spikes") was recorded in 96% (25/26) of ligatured ganglia prior to the motor neuron bursts. These spikes did not reach the threshold for inclusion in the "burst" due to their lower frequency. These leading spikes were quantified separately as a characteristic of the ligatured motor neuron patterned output. Data were analyzed statistically and graphed using Prism, version 7.0 (GraphPad Software, San Diego, CA, USA). Of the 26 preparations in which the CG survived the tightening of the ligature, 18 were used for myosuppressin application and assessment of baseline burst characteristics of the ligatured ganglion, as well as for assessing the re-patterning time of the ligatured neuron types. To standardize for variation in baseline, values are presented as percent change

add space between # and unit

from baseline; only preparations that returned to baseline during the saline wash after peptide application were included in the analysis. The ROUT method for identifying outliers (Motulsky and Brown 2006) was applied using Prism. One-sample t-tests were used to determine if the percentage change from baseline was significantly different from a hypothetical value of zero. Comparisons of two groups were done using Mann-Whitney tests. To compare more than two groups, ANOVAs were used, followed by Tukey post-hoc tests. P-values of < 0.05 were considered significant. N-values for all experiments refer to individual animals. All error values for physiological data represent standard deviation (SD).

In silico **identification of putative** ***Homarus americanus*** **myosuppressin signaling systems**

Database searches

Searches to identify transcripts encoding putative *H. americanus* myosuppressin precursors and receptor proteins were conducted with a workflow used previously for the identification of a variety of peptide precursors and receptors in this species, including those for myosuppressin (Christie et al. 2015; Christie et al. 2017). Specifically, the database of the online program tblastn (National Center for Biotechnology Information, Bethesda, MD; http://blast.ncbi.nlm.nih.gov/Blast.cgi) was set to Transcriptome Shotgun Assembly (TSA) and restricted to data from four lobster neural-specific transcriptomes: BioProject Nos. PRJNA300643 (mixed nervous system regions [brain, abdominal nerve cord, stomatogastric nervous system (STNS) and CG]; (Northcutt et al. 2016)), PRJNA338672 (eyestalk ganglia-specific; (Christie et al. 2017)), PRJNA379629 (brain-specific; (Christie et al. 2018a), and PRJNA412549 (CG-specific; (Christie et al. 2018b). missing paranthesis missing paranthesis In searches for transcripts encoding putative myosuppressin precursors (which were limited to the CG-specific transcriptome), a previously identified *H. americanus* myosuppressin preprohormone (Accession No. ACX46385; Stevens et al. 2009) was used as the query protein. In searches for putative *H. americanus* myosuppressin receptor-encoding transcripts, a previously predicted *Homarus* receptor (renamed here

MSR-I; deduced from Accession No. GEBG01049137; Christie et al., 2015) was used as the query sequence.

Identification of myosuppressin peptide and precursors

The putative mature structures of the *H. americanus* CG myosuppressin and myosuppressin precursor-related peptides were predicted using a workflow employed previously for peptide discovery in this species, including myosuppressin in other portions of the nervous system (Christie et al. 2015; Christie et al. 2017). In brief, BLAST hits were translated using the Translate tool of ExPASy (http://web.expasy.org/translate/) and assessed for the presence of a signal peptide using the online program SignalP 3.0 (http://www.cbs.dtu.dk/services/SignalP/; (Bendtsen et al. 2004). Prohormone cleavage sites were identified based on homology to known myosuppressin preprohormone processing schemes (Christie et al. 2015; Christie et al. 2017). The sulfation state of tyrosine residues and disulfide bonding between cysteine residues were predicted using the online programs Sulfinator (http://www.expasy.org/tools/sulfinator/; onigatti et al. 2002)) and DiANNA (http://clavius.bc.edu/~clotelab/DiANNA/; Ferre and Clote 2005). Cyclization of N-terminal glutamine residues and C-terminal amidation at glycine residues were predicted by homology to mass-spectrally identified decapod myosuppressin isoforms (Stemmler et al. 2007).

Identification and vetting of candidate receptors

Candidate myosuppressin receptors were predicted and vetted using a workflow that previously identified putative peptide receptors in a variety of decapod species, including *H. americanus* (Christie et al. 2015; Christie and Yu 2019; Dickinson et al. 2019b). Specifically, nucleotide sequences were translated using the Translate tool of ExPASy (http://web.expasy.org/translate/) and assessed for completeness. Next, each *H. americanus* receptor was used as the input query in a BLAST search of the annotated *Drosophila melanogaster* proteins curated in FlyBase (version FB2019_06; http://flybase.org/blast/index.html; Thurmond et al. 2019). This workflow was conducted on or before January 14, 2020. Finally, protein structural motifs were predicted for each

of the *H. americanus* receptors using the online program Pfam (version 32.0; http://pfam.xfam.org; El-Gebali et al. 2019). Transmembrane domains were predicted using the TOPCONS web server (Tsirigos et al., 2015).

missing parantheses

Amino acid alignments and calculations of amino acid identity/similarity

Amino acid alignments were done using the online program MAFFT (version 7; http://mafft.cbrc.jp/alignment/software/; Katoh and Standley 2013). Amino acid identity/similarity between putative peptide receptors was calculated using the MAFFT alignment outputs. Specifically, percent identity was calculated as the number of identical amino acids divided by the total number of residues in the longest sequence (x100), while amino acid similarity was calculated as the number of identical and similar amino acids divided by the total number of residues in the longest sequence (x100).

missing parantheses

Phylogenetic analysis of Homarus *myosuppressin receptors*

Phylogenetic relationships between the putative *H. americanus* myosuppressin receptor sequences and defined *D. melanogaster* peptide receptors were inferred from a multiple sequence alignment constructed using default MUSCLE (Edgar 2004) settings in Geneious (version 10.1.3; Biomatters Ltd., Auckland, New Zealand; Kearse et al. 2012). Evolutionary analyses were conducted in MEGA X (Kumar et al. 2018) using the maximum likelihood method based on the Le and Gascuel (2008) model. Initial tree(s) for the heuristic search were obtained automatically by applying Neighbor-Joining and BioNJ algorithms to a matrix of pairwise distances estimated using the Jones-Taylor-Thornton model (Jones et al., 1992), and then selecting the topology with superior log likelihood value. A discrete Gamma distribution was used to model evolutionary rate differences among sites (5 categories (+*G*, parameter = 1.2975)). The resulting tree was drawn to scale with bootstrap support from 1000 iterations indicated at branch nodes and branch lengths measured in terms of substitutions per site. The analysis involved 40 amino acid sequences. All positions with less than 95% site coverage were eliminated such that fewer than 5% alignment gaps, missing data, and ambiguous bases were allowed at any position; the final dataset consisted of 287 positions. Phylogenetic inferences made using neighbor joining (Saitou and Nei 1987) and minimum evolution

missing parantheses

(Rzhetsky and Nei 1992) approaches generated trees with similar topologies. Accession numbers for sequences used in the phylogenetic analyses are provided in Supplemental Table 1 (https://zenodo.org/record/3678732#.XlBhjChKhPY).

Reverse-transcriptase PCR (RT-PCR)

Myosuppressin receptor cloning

To facilitate cloning of the putative *H. americanus* myosuppressin receptors, total RNAs were purified from individual brains and eyestalk ganglia pairs (n = 3 independent samples from each tissue) as described previously (Christie et al. 2017; Christie et al. 2018a). RNA quality and quantity were assessed using an Agilent 2100 Bioanalyzer (Agilent Technologies, Santa Clara, CA, USA). cDNAs were synthesized from ~500 ng of total RNA with random pentadecamers (IDT, San Diego, CA, USA) and a SuperScript III First-Strand Synthesis System (Life Technologies Corp.). Full-length transcripts corresponding to MSR-I, II, and V were amplified using the respective cDNAs with SapphireAmp Fast PCR Master Mix (Takara Bio USA, Inc., Mountain View, CA, USA) and oligonucleotide primers (Table 1) designed to span the respective open reading frames (ORFs). PCR was performed in a 20 µL reaction volume with 0.5 µL cDNA and thermocycler conditions consisting of 95°C for 2 min, followed by 40 cycles of 95°C for 20 s, 56°C for 20 s, and 72°C for 2 min, with a final extension at 72°C for 5 min. Overlap extension PCR (Wurch et al. 1998) was used to amplify the MSR-IV ORF with oligonucleotide primers designed to stagger the MSR-IV coding sequence (Table 1). PCR was performed as before with SapphireAmp Fast PCR Master Mix in a 20 µL reaction volume with 0.5 µL cDNA and initial thermocycler conditions consisting of 95°C for 2 min, followed by 37 cycles of 95°C for 20 s, 56°C for 20 s, and 72°C for 1 min, with a final extension at 72°C for 5 min. The respective products were then used as templates for a second round of PCR using primers designed to span the putative ORF and thermocycler conditions consisting of 95°C for 2 min, followed by 27 cycles of 95°C for 20 s, 56°C for 20 s, and 72°C for 1:25 min, with a final extension at 72°C for 5 min. The *H. americanus* MSR-III sequence predicted in the transcriptomic assembly is a 3' fragment that lacks an identifiable start codon. Consequently, primers (Table 1) were

designed to amplify a 931-bp portion of the fragment that included the putative stop codon. PCR was performed as before with 0.5 µL cDNA and thermocycler conditions consisting of 95°C for 2 min, followed by 40 cycles of 95°C for 20 s, 58°C for 20 s, and 72°C for 1 min, with a final extension at 72°C for 5 min. All PCR products were visualized on 1.5% agarose gels stained with SYBR Safe (Life Technologies Corp.), sub-cloned into pCR2.1TOPO TA (Life Technologies Corp.) and sequenced at the Arizona State University DNA Core laboratory (Tempe, AZ, USA). Consensus sequences for the cloned MSR transcripts have been deposited in GenBank under Accession Nos. MT068477-MT068483.

Myosuppressin cloning

To clone the *H. americanus* myosuppressin preprohormone coding sequence, total RNAs were purified from isolated complete CGs as described previously (Christie et al. 2018b) and then treated with DNase I (New England Biolabs, Ipswich, MA, USA) for 10 min at 37°C to remove contaminating genomic DNA. cDNAs were synthesized using a SuperScript III First-Strand Synthesis System (Life Technologies) from ~100 ng total RNA with random pentadecamers (IDT). The myosuppressin preprohormone was amplified with SapphireAmp Fast PCR Master Mix (Takara Bio USA, Inc.) and oligonucleotide primers (Table 1) designed to the ORF in the deposited *H. americanus* myosuppressin preprohormone mRNA sequence (Accession No. GQ303179). PCR was performed in a 20 µL reaction volume with 0.5 µL cDNA and thermocycler conditions consisting of 95°C for 2 min, followed by 40 cycles of 95°C for 20 s, 56°C for 20 s, and 72°C for 30 s, with a final extension at 72°C for 5 min. The PCR product was visualized, sub-cloned, and sequenced as above.

Transcript expression profiling

To examine expression of the myosuppressin and MSR transcripts, total RNAs were purified from the premotor and motor neuron regions of the CG. Each CG was cut just posteriorly of motor neuron 5 to separate all premotor and motor and neuron cell bodies. For each sample, tissue from 10 ganglia was pooled (n = 6 pooled biological replicates for premotor neurons; n = 7 for motor neurons). RNA purification was performed using a

Takara NucleoSpin XS RNA isolation kit (Takara Bio USA, Inc.) with on-column rDNase treatments based on manufacturer protocols. Prior to storage at –80°C, RNA quantity and quality were assessed with an Agilent 2100 Bioanalyzer (Agilent Technologies, Santa Clara, CA, USA) or an Agilent 4150 TapeStation System (Agilent Technologies) with RNA ScreenTape analysis. cDNAs were synthesized from premotor and motor neuron tissue RNA (2 – 82 ng of total RNA) as above with random pentadecamers. The myosuppressin preprohormone transcript was amplified using primers that spanned the full ORF, whereas the respective MSRs were amplified using primers designed to amplify 500-bp fragments of each transcript (Table 1). Amplification was performed with SapphireAmp Fast PCR Master Mix (Takara Bio USA, Inc) in a 20 µL reaction volume with 0.8 µL cDNA and thermocycler conditions consisting of 95°C for 2 min, followed by 40 cycles of 95°C for 20 s, 56°C for 20 s, and 72°C for 30 s, with a final extension at 72°C for 5 min. The PCR product was visualized, sub-cloned, and sequenced as above. To confirm the suitability of the respective primer sets for amplification, aliquots of brain and eyestalk ganglia, described above, were also profiled using the same conditions as the premotor and motor neuron regions. To verify the integrity of the cDNA templates, a 500-bp fragment of the *H. americanus* glyceraldehyde-3-phosphate dehydrogenase (GAPDH) housekeeping gene (Accession No. FE043664) was likewise amplified. PCR products were separated on 1.5% agarose gels and visualized as before with representative amplicons sub-cloned and sequence verified. Gel images were obtained using an Azure 200 Gel Imaging Workstation (Azure Biosystems, Dublin, CA) and then processed in Photoshop CS6 v13.0 (Adobe Systems Inc., San Jose, CA).

RESULTS

After the CG had been removed from the surrounding musculature, the isolated ganglion always displayed regular bursting activity. Control activity of the isolated CG consisted of spontaneous, coupled bursting activity. Motor neuron output was monitored distally of motor neurons 1 and 2 on the anterolateral nerves. Although Hartline (1967) reported that premotor axons do not extend distally from these motor cell bodies, in 19% (5/26) of

recordings, premotor neuron spikes were recorded from this region of the ganglion. The well on the posterior trunk consistently captured both premotor and motor neuron activity in the intact CG where axons for both neuronal types overlap in the ganglionic trunk (Hartline 1967). Sorting the recorded action potentials by size allowed for analysis of the neuronal firing pattern. In the intact CG, premotor and motor neuron activity was in-phase (Figure 2A). Premotor bursts began milliseconds before and always ended after the motor neuron bursts, but the bursts ended at variable phases, as previously described (Cooke 2002; Mayeri 1973; Williams et al. 2013). Thus, premotor bursts were longer than the coupled motor bursts (Figure 2A).

The ligature is an effective method to separate the premotor and motor neurons

To understand the different neuronal components of the CG, the ligature placed prior to experimentation was tightened to physically decouple the premotor and motor neurons. Separation of cell types by ligature was an effective method to physically decouple premotor and motor neurons. Tying a small knot from a single strand of 6-0 suture silk did not obstruct superfusion and caused minimal damage to the cell bodies and axons. Placement of the ligature anterior to the fourth motor neuron allowed the spike initiation zones of the premotor axons to remain intact while the neuronal types were decoupled (Figure 1B). To ensure that the ligature was an effective method of separating the neuronal types, we cut the ganglion after tightening the ligature in several preparations. When the ganglionic trunk was cut (data not shown) just posterior to the ligature, motor neuron bursting continued without an injury discharge (n = 3). When the cut was made just anterior to the ligature, premotor neuron bursting was undisrupted (n = 3), indicating that the ligature effectively separated the two regions of the CG.

The ligatured cardiac ganglion re-establishes bursting activity in both the premotor and motor neurons

Following tightening of the ligature, the coordinated bursting activity characteristic of the intact CG was abolished, replaced by uncoupled, spontaneous neuronal output (Figure

2B). The pin electrode on the anterolateral nerve recorded only motor neuron output and the pin electrode on the trunk recorded only premotor neuron activity. Of 41 ligatured experiments attempted, both the premotor and motor neurons re-established an observable bursting pattern in 26 CGs (63.4%). However, the baseline firing pattern of both the premotor and motor neurons changed relative to their intact firing pattern (Figure 2).

In the 18 preparations in which myosuppressin was applied to the intact and ligatured CG, changes in baseline burst duration and frequency induced by ligature tightening were examined across both neuron types (Figure 3). The duration of bursts in the ligatured motor neurons was shorter than that of bursts in the motor neurons in the intact CG (0.24 s ± 0.07 s vs. 0.4 s ± 0.2 s; $p = 0.0042$). In contrast, the burst duration of the premotor neurons did not change with the ligature (0.63 s ± 0.19 s vs. 0.6 s ± 0.2 s; $p = 0.9757$). The burst frequency of ligatured motor neurons was significantly lower than that of the motor neurons in the intact CG (0.32 Hz ± 0.09 Hz vs. 0.40 Hz ± 0.11 Hz; $p = 0.0338$), but the frequency of bursting in the premotor neurons did not change with the tightening of the ligature (0.40 Hz ± 0.11 Hz vs. 0.47 Hz ± 0.12 Hz; $p = 0.1123$).

In the ligatured CG, the duration of premotor neuron bursts was longer than that of the motor neuron bursts (0.6 s ± 0.2 s vs. 0.24 s ± 0.07 s; $p < 0.0001$). In contrast, burst frequency, which was identical in the two neuronal types in the intact ganglion, was higher in the ligatured premotor neurons than in the ligatured motor neurons (0.47 Hz ± 0.12 Hz vs. 0.32 Hz ± 0.09 Hz; $p = 0.0005$). Additionally, leading spikes were recorded in 96% (25/26) of ligatured ganglia prior to the motor neuron bursts. Similar leading spikes were recorded in 19% (5/26) of ligatured premotor neurons (Figure 2B).

Across all 18 preparations in which bursting was recorded as the ligature was tightened and during the re-establishment of bursting in the two neuronal types, there was considerable variability in the time required to re-establish bursting in the two neuron types (means: motor: 4.33 min ± 8.48 min, premotor: 10.47 min ± 13.51 min; paired t-test, $p = 0.1346$, $n = 18$). In 13 of the 18 preparations, the bursting pattern was re-

established more quickly in the motor neurons than in the premotor neurons (binominal test, $p = 0.049$). In three preparations, the post-ligature pattern was established immediately in both cell types. In the remaining two preparations, post-ligature bursting was established more quickly in the premotor neurons. In 36.5% (15/41) of preparations, a strong post-ligature burst pattern was never achieved; of these 15 CGs, four (9.8%) demonstrated no bursting in either cell type after the ligature. Of the eleven ganglia in which only one neuron type re-established a bursting pattern, motor neurons achieved a post-ligature burst pattern in five CGs, while the premotor neurons re-established bursting in the other six CGs.

Myosuppressin modulates cardiac ganglion output

Application of myosuppressin to the isolated, but intact, CG resulted in observable changes in burst characteristics (Figure 4), consistent with previous reports (Stevens et al. 2009). In order to quantify the effects of myosuppressin, burst characteristics, including burst frequency, interburst interval, and burst duration, were measured at the time of peak response to the peptide. To enable comparison between CGs with different baseline firing patterns, data were normalized by comparing percent change from baseline (Figure 5A-F). When superfused over the intact CG at a concentration of 10^{-7} M, myosuppressin elicited a decrease in burst frequency (Figure 5A, $p = 0.0058$ for both cell types) and an increase in interburst interval (Figure 5B, $p = 0.0332$ for premotor neurons, $p = 0.0365$ for motor neurons). No change in burst duration was observed for either motor or premotor neurons (Figure 5C). When superfused at 10^{-6} M, myosuppressin also elicited a decrease in burst frequency (Figure 5D, $p < 0.0001$ for both cell types) and an increase in interburst interval (Figure 5E, $p = 0.0022$ for premotor neurons, $p = 0.0021$ for motor neurons) in both cell types. Additionally, the peptide elicited a large increase in burst duration in both neuronal types (Figure 5F, $p = 0.0030$ for premotor neurons, $p = 0.0014$ for motor neurons). All observed changes in burst characteristics resulting from 10^{-6} M peptide application were larger in magnitude than those elicited in response to 10^{-7} M application ($p < 0.05$).

Application of myosuppressin to the ligatured CG enabled us to determine whether the peptide exerted independent modulatory effects on the premotor and motor neurons of the CG. Myosuppressin superfused at both 10^{-7} M and 10^{-6} M altered specific aspects of the bursting pattern in both the premotor and motor neurons (Figure 4). Although 10^{-7} M myosuppressin elicited a decrease in burst frequency in both neuronal types when the CG was intact, in the ligatured CG, burst frequency was decreased only in the motor neurons (Figure 5A, $p < 0.0001$ for motor neurons, $n = 8$); 10^{-7} M myosuppressin did not significantly change burst frequency in the premotor neurons (Figure 5A, $p = 0.3045$, $n = 8$). When myosuppressin was superfused over the ligatured CG at a higher concentration (10^{-6} M), a decrease in burst frequency during myosuppressin application was observed in both neuron types (Figure 5D, $p < 0.0001$ for both premotor and motor neurons, $n = 10$).

When superfused at 10^{-7} M, myosuppressin elicited a significant increase in interburst interval only in the ligatured motor neurons (Figure 5B, $p = 0.0018$), while an increase had been observed in both cell types in the intact CG. However, an increase in interburst interval was observed in both cell types at a concentration of 10^{-6} M (Figure 5E, $p = 0.0033$ for premotor neurons, $p = 0.0075$ for motor neurons), as in the intact ganglion.

As was the case in the intact ganglion, 10^{-7} M myosuppressin did not alter burst duration in either the ligatured premotor or motor neurons, although an increase in burst duration was observed in the ligatured premotor neurons in the presence of 10^{-6} M myosuppressin (Figure 5C/F, $p < 0.0001$ for premotor neurons). However, 10^{-6} M myosuppressin failed to elicit a change in burst duration in the motor neurons, which contrasts with its effects in the intact ganglion, where it elicited an increase in burst duration in both premotor and motor neurons.

While changes in various burst characteristics were observed across the cell types at the peak response to the peptide, the time course of these alterations to the bursting pattern differed between the two neuronal types (Figure 6). At a concentration of 10^{-6} M, the onset of the characteristic decrease in burst frequency observed in the motor neurons was gradual across the period of peptide application. The onset of this gradual decrease

consistently preceded the large increase in burst duration observed in the premotor cells. The number of leading spikes that preceded ligatured motor neuron bursts was not significantly altered by myosuppressin application at 10^{-6} M or 10^{-7} M.

Taken together, these data suggest that myosuppressin exerts distinct and concentration-dependent effects on the premotor and motor neurons of the CG. These data raise two additional questions. First, having noted that the peptide concentrations that elicit these effects are concentrations typically associated with local rather than hormonal release (Dickinson et al. 2015), we asked whether myosuppressin might be produced locally in the CG. Second, given the different responses to myosuppressin in the two neuronal types, and the fact that multiple myosuppressin receptors have been identified in at least some arthropod species (Dickinson et al. 2019b; Egerod et al. 2003), we asked whether multiple myosuppressin receptors are expressed in the lobster nervous system, and if so, whether they are differentially distributed across the two neuronal types.

In silico identification of myosuppressin as a neuropeptide produced in the cardiac ganglion of _Homarus americanus_

The threshold concentrations for the myosuppressin effects reported here were 10^{-7} or 10^{-6} M, concentrations typically associated with locally released peptide. While several peptides have been identified previously in the *H. americanus* CG (Christie et al. 2010b; Dickinson et al. 2018; Dickinson et al. 2015), including at least one, diuretic hormone 31, synthesized by the motor neurons (Christie et al. 2010b), the presence of myosuppressin within the ganglion has not been investigated. Here, using a previously identified *Homarus* prepro-myosuppressin sequence (Stevens et al. 2009), the *H. americanus* CG-specific assembly was searched for transcripts encoding putative homologs. This search returned three transcripts (Accession Nos. GGPK01064738-GGPK01064740) that encode the same 100 amino acid full-length preprohormone. The putative CG prepro-myosuppressin is identical to that identified initially by Stevens et al. (2009), and is predicted to give rise to four peptides: the myosuppressin isoform pQDLDHVFLRFamide, and the linker/precursor-related peptides

554 VCVGVGETMPPPICLSQQVPLSPFA (disulfide bridging between the two cysteine
555 residues), LCSALINISEFSRAMEEY$_{(SO3H)}$LGAQAIERSMPVNEPEV, and SQQ.
556 Furthermore, multiple clones with > 99% nucleotide (nt) identity to the *in silico* derived
557 transcripts were amplified from CG-specific cDNAs.
558
559 **Identification of five candidate *Homarus americanus* neuronal myosuppressin**
560 **receptors**
561
562 Prior to the study presented here, a single putative myosuppressin receptor had been
563 reported from *H. americanus* (Christie et al. 2015). This receptor (renamed here MSR-I;
564 Figure 7) was predicted from a transcript identified via a BLAST search of a *H.*
565 *americanus* mixed nervous system region transcriptome using a *D. melanogaster* MSR as
566 the input query (Christie et al. 2015). Because a BLAST search of the *Homarus* CG-
567 specific assembly failed to identify any transcripts encoding this protein (Table 2 and
568 Supplemental Table 1; https://zenodo.org/record/3678732#.XlBhjChKhPY), we
569 hypothesized that additional receptors for myosuppressin must be present in *H.*
570 *americanus*, including in the CG. Reassessment of the mixed nervous system assembly,
571 as well as searches of brain-, eyestalk ganglia-, and CG-specific transcriptomes,
572 identified sequences encoding four additional candidate *H. americanus* MSRs (MSR-II-
573 V; Figure 6 and Supplemental Table 2;
574 https://zenodo.org/record/3678732#.XlBhjChKhPY). Unlike *Homarus* MSR-I,
575 whose top FlyBase annotated *D. melanogaster* protein hit is isoform B of myosuppressin
576 receptor 1 (Accession No. AGB94019), MSR-II-V returned uncharacterized protein
577 Dmel_CG13229 (Accession No. AGB94019) as the most similar protein. Although it
578 was originally identified as a putative *D. melanogaster* myosuppressin receptor,
579 CG13229 was not activated by the native *Drosophila* myosuppressin isoform, at least in
580 the expression system/bioassay that was used for receptor deorphanization (Hauser et al.
581 2006). Regardless, all four of the new candidate *H. americanus* MSRs are similar in
582 amino acid sequence to MSR-I (Table 3) and possess a single serpentine receptor class W
583 seven-transmembrane domain (Figure 7), a domain also present in *Homarus* MSR-I and
584 *D. melanogaster* myosuppressin receptor 1 and CG13229. Furthermore, the putative

Homarus MSRs cluster in an MSR-specific clade with the *Drosophila* proteins in which the CG13229 sequence forms a well-supported branch with the *Homarus* MSR-IV and V proteins (Figure 8). While transcripts encoding *H. americanus* MSR-I-V were found in the mixed nervous system, brain-specific, and eyestalk ganglia-specific transcriptomes, evidence of expression for only MSR-II-IV was found in the CG-specific assembly (Table 2 and Supplemental Table 1; https://zenodo.org/record/3678732#.XlBhjChKhPY). Clones amplified from brain and eyestalk ganglia cDNAs for MSR-I and II exhibited > 99% nt identity with the transcriptomic sequences, as did partial clones comprising a 931-bp portion of the MSR-III 3' fragment. Three MSR-IV variants (referred to as MSR-IV v1-3) were amplified from the brain and eyestalk ganglia cDNAs. MSR-IV v1 has > 99% nt identity, whereas MSR-IV v2 has a 42 nt deletion (nt 1172-1213) in the C-terminal coding sequence, but retains the full-length variant reading frame for the terminal seven amino acids and stop codon. MSR-IV v3 has a 312 nt deletion (nt 902-1213) that results in loss of the last two transmembrane domains, but likewise retains the terminal seven amino acids and stop codon. The MSR-V clones obtained from the brain and eyestalk ganglia cDNAs contained a 1425 nt ORF that differed from the transcriptomic sequence by a 36 nt insertion at nt 1058 that maintained the same reading frame over the final 332 nucleotides. Consensus validated sequences for all MSRs have been deposited with GenBank under Accession Nos. MT068477-MT068483.

Differential expression of myosuppressin receptors between neuronal types in the cardiac ganglion may underlie physiological response to local myosuppressin release

Previous and current physiological data suggest local release of myosuppressin, which is consistent with the presence of its transcript in a CG-specific transcriptome assembly. To assess transcript expression in the two CG neuron types, we performed RT-PCR using premotor and motor neuron-specific cDNAs from multiple biological replicates as well as cDNA from brain and eyestalk ganglia. As expected, amplicons corresponding to the prepropeptide were generated from all tissues examined (Figure 9A), albeit at differing

615 intensities from the CG region-specific cDNAs, which could indicate region-specific
616 transcriptional control.
617
618 Given the presence of five putative myosuppressin receptor transcripts in the lobster
619 nervous system, we asked whether any were expressed in the CG, and if so, whether they
620 were expressed differentially in mRNA isolated from the premotor and motor regions of
621 the ganglion. First, to examine the ability of our expression profiling primers to amplify
622 the five putative receptor transcripts, we confirmed amplification of 500-bp fragments
623 from *H. americanus* brain and eyestalk ganglia cDNAs (Figure 9B); for MSR-IV, which
624 consists of at least three variants (i.e., MSR-IV v1-3), the primers used were designed to
625 amplify a conserved portion of the respective variant sequences.
626
627 RT-PCR profiling of the CG region cDNAs showed that, similar to the CG transcriptomic
628 data, transcripts encoding MSR-I and MSR-V are either not present in the two neuron
629 types or are expressed at levels below the threshold of detection (Figure 9B). Although
630 the RT-PCR data shown here are not quantitative, we can compare relative intensities of
631 the bands for each of the receptors, using the GAPDH housekeeping gene as a baseline.
632 Intensities of the GADPH bands are relatively constant across samples, suggesting that
633 large differences between expression in the different neuronal types may reflect
634 differences in receptor expression levels. Our results suggest that MSR-II is either motor
635 neuron-specific or that it is expressed in much higher levels in the motor neurons than in
636 the premotor neurons. Across the six pooled replicates of the premotor neurons, MSR-II
637 appeared at low expression levels in just one pooled sample, whereas it was prominent in
638 all of the motor neuron samples.
639
640 Both MSR-III- and MSR-IV-encoding transcripts were present in multiple tissue
641 replicates for both neuron types. RT-PCR results suggest that MSR-III is more abundant
642 in the motor neurons than the premotor neurons (amplicon present in all six pooled motor
643 neuron replicates vs. two of six premotor neuron replicates). In contrast, MSR-IV
644 appeared to be expressed predominantly in the premotor neurons rather than the motor

neurons (amplicon present in all six pooled replicates vs. four of seven motor neuron replicates).

DISCUSSION

The rhythmicity of neuronal firing observed in the lobster CG has been characterized as an exemplary model of a circuit with a grouped pacemaker configuration (Cooke 2002). In the classical view of the CG, pacemaker potentials that originate in the four small premotor neurons transmit their synchronized activity to the larger motor neurons via excitatory synapses and electrical connections to initiate motor neuron firing. The chemical and electrical coupling of these cell types is complex and raises the question as to whether cross-neuronal communication can be fully blocked.

The components of the CG: the physically decoupled premotor and motor neurons

To examine the physically decoupled premotor and motor neurons, we used a physical ligature to disrupt the coordinated, in-phase bursting of the premotor and motor neurons. Previously, when the motor neurons were separated from the premotor neurons and voltage clamped, the driver potentials were shown to consist of an inward calcium current and three outward potassium currents, but no pacemaking currents were identified (Tazaki and Cooke 1990; 1986). Both motor neurons 1 and 2, when individually isolated by ligature, were able to respond to imposed depolarizing pulses with driver potentials, but were quiescent in the absence of stimulation (Tazaki and Cooke 1983). However, studies demonstrated that transected *Homarus* ganglion segments containing motor neuron soma were capable of producing rhythmic bursting (Mayeri 1973; Tazaki and Cooke 1983). Mayeri noted that when bursting was present, impulses attributable to small cell axons included in the isolated nerve segment were detected in addition to large axon impulses (Mayeri 1973). Tazaki and Cooke (1983) observed rhythmic spontaneous burst generation from motor neuron 3 after isolation of the ganglion segment containing its soma and proximal axons by three ligatures. However, they did not routinely monitor the extracellular activity of the isolated nerve segments; thus, the potential participation of

676 premotor neuron processes was unknown (Tazaki and Cooke 1983). While we cannot
677 rule out the potential interaction between motor neurons and inactive premotor neuron
678 axons that could contribute to the observed bursting, our placement of the ligature
679 anterior to the soma of motor neuron 4 meant that no active premotor neuron axons were
680 present (Hartline 1967), which was confirmed by extracellular recordings in which small
681 axon impulses were absent. This suggests that the observed rhythmic bursting of the
682 motor neurons is attributable to the intrinsic neuronal properties of one or more motor
683 neurons. Here, we report that the premotor and motor neurons of the ganglion can
684 establish independent bursting patterns in about 2/3 of preparations that have been
685 physically decoupled by a ligature. These results suggest that the isolated motor neurons
686 can possess intrinsic bursting properties that explain their firing pattern when decoupled
687 from the premotor neurons.
688
689 In further characterization of the inward currents and channels underlying bursting
690 activity of *Cancer borealis* CG neurons, Ransdell et al. (2013) identified a largely non-
691 inactivating TTX-sensitive current necessary for driver potential generation, which
692 suggested the presence of a persistent sodium current, I_{NaP}. Such currents have been
693 shown to alter the bursting frequency and contribute to the burst generating ability of
694 pacemaker neurons. In the DG neurons of the spiny lobster, *Panulirus interruptus*,
695 stomatogastric ganglion (STG), the presence of I_{NaP} is known to be important in plateau
696 potential generation (Elson and Selverston 1997) and a TTX-sensitive persistent sodium
697 current has been identified in cultured *P. interruptus* STG cells (Turrigiano et al. 1995).
698 Additional evidence in mammalian pre-Bötzinger neurons has shown that I_{NaP} is
699 necessary for burst generation (Del Negro et al. 2002a; Del Negro et al. 2002b).
700 Therefore, it is possible that the presence of a persistent sodium current in one or more of
701 the *H. americanus* motor neurons may explain their independent bursting capability
702 observed here. Variable expression of different currents across individuals, as seen in
703 crabs (Ransdell et al. 2013), might underlie the variability of the responses to the ligature
704 across animals.
705

706 Across all ligatures attempted, over 30% (15/41) of preparations did not re-establish
707 bursting in both the premotor and motor neurons. Since we did not conduct intracellular
708 or voltage clamp recordings, we cannot determine the mechanism that underlies this
709 variability. However, recent appreciation for variation in neuronal parameters such as
710 synaptic strengths (Grashow et al. 2010; Olypher and Calabrese 2007; Wilhelm et al.
711 2009), conductance magnitudes (Schulz et al. 2006; Wilhelm et al. 2009), and channel
712 activation properties (Amendola et al. 2012) that underlie identical patterned output
713 across neurons suggest that multiple mechanisms may contribute to the CG bursting
714 examined here. It is possible that in some CGs, the mechanisms that are important for
715 burst generation in one or both neuron types are more resilient and able to function in
716 isolation from the rest of the network, while in others, cross-neuronal interactions are
717 more critical to the maintenance of bursting activity.
718
719 Ligaturing the CG did not significantly alter the duration or frequency of premotor
720 neurons bursts, but significantly increased the duration and decreased the frequency of
721 motor neuron bursts; it also introduced a trail of leading spikes into these neurons. In the
722 ligatured CG, the intrinsic burst duration and frequency of the premotor and motor
723 neurons differed significantly from one another. In a two-cell model of the *Homarus* CG
724 derived from Morris-Lecar oscillators (Morris and Lecar 1981), the two neuron types
725 displayed different intrinsic duty cycles (Williams et al. 2013). Across model runs, the
726 neurons were drawn towards a compromise value via synaptic coupling and predicted
727 strong electrical coupling as a key mediator of burst synchronization between
728 heterogeneous oscillators. The data gathered here provide further evidence for neuronal
729 heterogeneity in this coupled network, as well as additional evidence that synchronization
730 between the premotor and motor neurons allows the premotor neurons to drive the
731 bursting pattern of the CG, as previously hypothesized (Hartline 1967). Moreover, the
732 ligatured burst characteristics observed here highlight the variability in network phasing
733 that might result from variation in strength of coupling between neuron types or in the
734 intrinsic burst characteristics.
735

736 Separating the motor and premotor neurons with a ligature induced leading spikes in
737 nearly all (25/26) of the ligatured motor neuron regions. Intracellular recordings would
738 enable us to see whether or not the characteristic leading spikes are due to a
739 depolarization of the membrane potential between driver potentials. However, this does
740 not seem likely, as depolarization of the motor neurons in an intact ganglion leads to a
741 higher burst frequency, whereas in the ligatured ganglion, the burst frequency decreases.
742 In a previous study, when proctolin was applied to a motor sensitive region of the
743 *Homarus* CG, a depolarization of the motor neurons was accompanied by an increase in
744 burst frequency (Miller and Sullivan 1981; Sullivan and Miller 1984). This suggests that
745 the leading spikes are due to a mechanism more complex than simple depolarization. One
746 possibility is that, when the ligature was tightened, and a spike-initiating zone was
747 removed, new spike initiation zones were established, including one that generated the
748 leading spikes. Such establishment of new spike-initiating zones has been observed in
749 esophageal neurons of the stomatogastric nervous system in the spiny lobster, *Jasus*
750 *lalandii*. These neurons have multiple spike initiating zones (Nagy et al. 1981); when cut,
751 they often establish additional, new spike-initiation zones (unpublished observations).
752
753 **Myosuppressin differentially modulates premotor and motor neurons in the CG**
754
755 Here, we assessed the effects of myosuppressin on the two neuron types in the lobster
756 CG. In both this and a previous study (Stevens et al. 2009), myosuppressin exerted clear
757 effects on the isolated and intact CG at concentrations of 10^{-6} to 10^{-8} M. The upper ranges
758 of the concentrations reported by Stevens (2009), however, are typically associated with
759 local rather than hormonal release (Dickinson et al. 2019a; Dickinson et al. 2015;
760 Messinger et al. 2005). For example, when FMRFamide-like peptides were measured
761 using a radioimmunoassay based on a FMRF-amide antibody in lobster, concentrations
762 from 10^{-11} to 10^{-10} M were reported in circulating hemolymph (Kobierski et al. 1987).
763 Hemolymph concentrations up to 3-4 x 10^{-8} M were reported for other circulating
764 peptides in insects and shrimp, including vitellogenenin inhibiting hormone and ecdysis-
765 triggering hormone (Fastner et al. 2007; Kang et al. 2014; Zitnan et al. 1999). However,
766 many of the effects of myosuppressin were observed only at concentrations higher than

hyphenate?

767 those associated with hormonal release of other neuropeptides. This, together with the
768 fact that myosuppressin transcripts were identified in both the premotor and motor neuron
769 regions of the CG (Figure 9A) suggests that the peptide may be locally released. Since
770 the premotor and motor neurons are connected by chemical synapses as well as electrical
771 coupling (Cooke 2002), it is feasible that myosuppressin released from the CG itself
772 could act as an intrinsic modulator (Katz 1995; Katz and Frost 1996) on both neuron
773 types. Another possible source for local myosuppressin release is the descending cardio-
774 regulatory fibers that innervate the CG (reviewed in Cooke 2002; Fort et al. 2004; Fort et
775 al. 2007). Because there are no antibodies specific to myosuppressin, it is not currently
776 possible to determine whether these pathways contain and release myosuppressin.
777 Together, these data suggest that the regulation of the heartbeat in the decapods may
778 involve integration of information from hormonal pathways, local release from
779 descending regulatory fibers, and release of modulators from intrinsic sources, suggesting
780 that central regulation of the heartbeat may be considerably more complex than
781 previously thought.

782 Stevens and colleagues (2009) examined the effects of myosuppressin in the intact
783 lobster, on the whole heart, on the isolated CG, and on the neuromuscular
784 junction/muscle. They determined that the global effects of myosuppressin on the cardiac
785 neuromuscular system represent the integration of site-specific effects. At concentrations
786 ranging from 10^{-8} M and 10^{-6} M, myosuppressin elicited a decrease in burst frequency,
787 but an increase in burst duration and contraction amplitude. The effects of myosuppressin
788 on the intact CG in our study are consistent with these previous findings. We investigated
789 whether these changes in burst duration and frequency are mediated by the premotor or
790 motor neurons, particularly in the isolated CG, in which no feedback is present. While
791 both 10^{-6} M and 10^{-7} M myosuppressin elicited changes in both ligatured neuron types,
792 the threshold for most of the changes we observed was 10^{-6} M. The only changes elicited
793 by 10^{-7} M myosuppressin in the ligatured ganglion were the decrease in burst frequency
794 and increase in interburst interval in the motor neurons, suggesting that the threshold for
795 effects of myosuppressin is lower in the motor neurons than it is in the premotor neurons.
796 The fact that 10^{-7} M myosuppressin is sufficient to elicit frequency changes in both

neuronal types when the CG is intact, but only in the motor neurons when ligatured suggests that the motor neurons play an important role in determining the burst frequency and interburst interval of the intact CG firing pattern, at least in the presence of low concentrations of myosuppressin. Myosuppressin might cause these changes by activating pathways that hyperpolarize the motor neurons, as was seen previously (Stevens et al. 2009), resulting in a decrease in burst frequency. Alternatively, it could also activate pathways that specifically affect the pacemaker potential, resulting in a slower rate of depolarization to the next burst.

In the intact CG, 10^{-6} M myosuppressin elicited an increase in burst duration that was not observed with 10^{-7} M peptide application. While neither concentration tested here elicited an increase in burst duration in the ligatured motor neurons, 10^{-6} M myosuppressin was capable of eliciting an increase in the burst duration of the ligatured premotor neurons. These data suggest that the premotor neurons are responsible for the increase in burst duration observed in the intact ganglion in response to 10^{-6} M myosuppressin.

The differential modulation by myosuppressin of the premotor and motor neurons suggests that the peptide may target different channels and currents in the two neuron types. In their characterization of the neurons of the *Homarus* CG, Tazaki and Cooke (1983) highlighted the role of driver potentials and a pacemaker potential in impulse generation. Given that myosuppressin appears to primarily alter the burst frequency of the isolated motor neurons, it is likely that myosuppressin targets a pacemaking potential in the motor neurons, such as the persistent sodium current previously identified in crab CG (Ransdell et al. 2013). Myosuppressin largely altered the burst duration of the isolated premotor neurons, suggesting that the peptide may target a different current or currents, specifically those implicated in the driver potentials, which underlie the bursts of action potentials in CG neurons, generated in this neuron type. If so, it appears that the sum of these interactions is what drives the changes in the patterned output of the intact CG.

826 Nonetheless, we cannot rule out the possibility that the application of myosuppressin to
827 ligatured preparations elicited effects that crossed the boundary that the ligature creates
828 between neuronal types. For example, if myosuppressin receptors are present in the
829 regions of the premotor neurons that remain in the motor neuron region after ligature,
830 those regions of the premotor neurons could be activated and influence the motor
831 neurons, and vice versa. The two neuronal types are tightly interconnected, so that
832 complete separation of the neuron types is impossible.
833
834 Although the motor neurons have previously been considered a relatively homogenous
835 set of neurons due to their tight electrical coupling, the data presented here do not provide
836 sufficient evidence to determine whether myosuppressin has the same effect on all motor
837 neurons. Intracellular recordings from the ligatured ganglion would provide further
838 information about the action of myosuppressin on individual motor neurons. The
839 appearance of the leading spikes, which appear to be singular action potentials generated
840 from a single neuron, raises the possibility that individual motor neurons may serve
841 distinct roles in the pattern generator output.
842
843
844 **Differential myosuppressin receptor distribution may contribute to differential**
845 **modulation of neuron types**
846
847 Recent advances in genomics/transcriptomics have enabled novel peptide identification
848 in a variety of animals, including crustaceans, and have prompted investigation of the
849 ability of neuropeptides to modulate rhythmic motor behaviors (Blitz 2017; Christie
850 2014a; b; c; Christie et al. 2011; Christie et al. 2010a; Dickinson et al. 2016). However,
851 published studies that examine the extent to which the differences in physiological effects
852 are related to differential receptor expression at the neuronal level are sparse. In the STG
853 of *C. borealis*, CCAP receptor expression was assessed, and expression levels differed
854 significantly between specific neuron types, in correlation with responses to the peptide
855 (Garcia et al. 2015). Here, we examined the expression of five myosuppressin receptor

transcripts (MSR-I-V) and found apparent differential expression across the premotor and motor neurons.

The predominant expression of MSR-II and MSR-III transcripts in the motor neurons relative to the premotor neurons (Figure 9B) is consistent with a potential role for MSR-II and MSR-III functionality in the decreased frequency that defines the bursting pattern of these neurons when ligatured. If MSR-II or MSR-III plays a similar role in all CG neurons, this would be consistent with the observation that the premotor neurons exhibit smaller changes in frequency with myosuppressin application, as MSR-II appears to have lower expression in the premotor neurons. Conversely, MSR-IV, which appears to be expressed at lower levels in the motor neurons, may primarily alter the driver potentials that define the burst duration of the coordinated ganglionic output. However, since mRNA can be trafficked throughout neurons, we cannot rule out the possibility that local mRNAs from premotor neuron presynaptic terminals or axons were collected with the motor neuron cell body tissue, or vice versa. Due to the intertwining of the axonal terminals and cell bodies, any separation of these neuron types is imperfect; in the procedure employed here, ganglionic tissue was divided to separate the premotor and motor neuron cell bodies, but terminals and axons were not fully separated.

CONCLUSIONS

The *Homarus americanus* cardiac neuromuscular system is a CPG-effector system that has been well studied at the level of the whole heart, the isolated CG (the CPG), and the isolated muscle (effector system). The patterned output can be modulated in response to an expansive class of neuropeptides, yet there remain few investigations of the CG at the level of the individual neuron types. In this work, we demonstrate that the premotor and motor neurons establish separate bursting patterns when decoupled by a physical ligature, and that their independent modulation by the neuropeptide myosuppressin may result from a differential distribution of myosuppressin receptors across neuron types.

887 Our results thus extend the literature on the *Homarus* CG, providing insight into the
888 cellular components of the CPG. Future work addressing the variable mechanisms that
889 may underlie the bursting capabilities of the separated neurons observed here would
890 further elucidate the role of each neuron type in producing coordinated ganglionic output.
891
892
893 **ACKNOWLEDGEMENTS**
894 Helen Gandler, Tess Lameyer, Micah Pascual, Devlin Shea, and Andy Yu are thanked for
895 their participation in early searches for lobster myosuppressin receptors. Jacob Kazmi is
896 thanked for assistance in extracting RNA. Dr. Colin Brent is thanked for reading and
897 commenting on an earlier draft of this manuscript. Funding was provided by the National
898 Science Foundation (IOS-1353023, IOS- 1354567), an Institutional Development Award
899 (IDeA) from the National Institute of General Medical Sciences of the National Institutes
900 of Health (P20GM103423), U.S. Department of Agriculture (USDA) base CRIS funding
901 (Project #2020-22620-022-00D), the Cades Foundation, the Henry L and Grace Doherty
902 Coastal Studies Research Fellowship, the Arnold and Mabel Beckman Foundation, and
903 the Paller Fund of Bowdoin College. Mention of trade names/commercial products in this
904 article is solely for the purpose of providing specific information and does not imply
905 recommendation/endorsement by the U.S. Department of Agriculture. USDA is an equal
906 opportunity provider/employer.
907

REFERENCES

Amendola J, Woodhouse A, Martin-Eauclaire M-F, and Goaillard J-M. Ca2+/cAMP-sensitive covariation of Ia and Ih voltage dependences tunes rebound firing in dopaminergic neurons. *The Journal of Neuroscience* 32: 2166-2181, 2012.

Bendtsen JD, Nielsen H, von Heijne G, and Brunak S. Improved prediction of signal peptides: SignalP 3.0. *Journal of molecular biology* 340: 783-795, 2004.

Berlind A. Feedback from motor neurones to pacemaker neurones in lobster cardiac ganglion contributes to regulation of burst frequency. *Journal of Experimental Biology* 141: 277-294, 1989.

Blitz DM. Circuit feedback increases activity level of a circuit input through interactions with intrinsic properties. *J Neurophysiol* 118: 949-963, 2017.

Brezina V. Beyond the wiring diagram: signalling through complex neuromodulator networks. *Philos Trans R Soc Lond B Biol Sci* 365: 2363-2374, 2010.

Briggman KL, and Kristan WB. Multifunctional pattern-generating circuits. *Annual review of neuroscience* 31: 271-294, 2008.

Christie AE. Identification of the first neuropeptides from the Amphipoda (Arthropoda, Crustacea). *Gen Comp Endocrinol* 206: 96-110, 2014a.

Christie AE. Peptide discovery in the ectoparasitic crustacean *Argulus siamensis*: identification of the first neuropeptides from a member of the Branchiura. *Gen Comp Endocrinol* 204: 114-125, 2014b.

Christie AE. Prediction of the peptidomes of *Tigriopus californicus* and *Lepeophtheirus salmonis* (Copepoda, Crustacea). *Gen Comp Endocrinol* 201: 87-106, 2014c.

Christie AE, Chi M, Lameyer TJ, Pascual MG, Shea DN, Stanhope ME, Schulz DJ, and Dickinson PS. Neuropeptidergic signaling in the American lobster *Homarus americanus*: new insights from high-throughput nucleotide sequencing. *PLoS One* 10: e0145964, 2015.

Christie AE, McCoole MD, Harmon SM, Baer KN, and Lenz PH. Genomic analyses of the *Daphnia pulex* peptidome. *Gen Comp Endocrinol* 171: 131-150, 2011.

Christie AE, Roncalli V, Cieslak MC, Pascual MG, Yu A, Lameyer TJ, Stanhope ME, and Dickinson PS. Prediction of a neuropeptidome for the eyestalk ganglia of the lobster *Homarus americanus* using a tissue-specific de novo assembled transcriptome. *Gen Comp Endocrinol* 243: 96-119, 2017.

Christie AE, Stemmler EA, and Dickinson PS. Crustacean neuropeptides. *Cellular and molecular life sciences : CMLS* 67: 4135-4169, 2010a.

Christie AE, Stevens JS, Bowers MR, Chapline MC, Jensen DA, Schegg KM, Goldwaser J, Kwiatkowski MA, Pleasant TK, Shoenfeld L, Tempest LK, Williams CR, Wiwatpanit T, Smith CM, Beale KM, Towle DW, Schooley DA, and Dickinson PS. Identification of a calcitonin-like diuretic hormone that functions as an intrinsic modulator of the American lobster, *Homarus americanus*, cardiac neuromuscular system. *The Journal of Experimental Biology* 213: 118-127, 2010b.

Christie AE, and Yu A. Identification of peptide hormones and their cognate receptors in J*asus edwardsii* – A potential resource for the development of new aquaculture management strategies for rock/spiny lobsters. *Aquaculture* 503: 636-662, 2019.

Christie AE, Yu A, Pascual MG, Roncalli V, Cieslak MC, Warner AN, Lameyer TJ, Stanhope ME, Dickinson PS, and Joe Hull J. Circadian signaling in *Homarus americanus*: region-specific de novo assembled transcriptomes show that both the brain and eyestalk ganglia possess the molecular components of a putative clock system. *Marine genomics* 40: 25-44, 2018a.

Christie AE, Yu A, Roncalli V, Pascual MG, Cieslak MC, Warner AN, Lameyer TJ, Stanhope ME, Dickinson PS, and Joe Hull J. Molecular evidence for an intrinsic circadian pacemaker in the cardiac ganglion of the American lobster, *Homarus americanus* - Is diel cycling of heartbeat frequency controlled by a peripheral clock system? *Marine genomics* 41: 19-30, 2018b.

Cooke IM. Reliable, responsive pacemaking and pattern generation with minimal cell numbers: The crustacean cardiac ganglion. *Biological Bulletin* 202: 108-136, 2002.

Del Negro CA, Koshiya N, Butera RJ, Jr., and Smith JC. Persistent sodium current, membrane properties and bursting behavior of pre-botzinger complex inspiratory neurons in vitro. *J Neurophysiol* 88: 2242-2250, 2002a.

Del Negro CA, Morgado-Valle C, and Feldman JL. Respiratory rhythm: an emergent network property? *Neuron* 34: 821-830, 2002b.

Delcomyn F. Even "simple" systems are more complex than we thick. *Behavioral and Brain Sciences* 3: 544, 1980.

Dickinson PS, Armstrong MK, Dickinson ES, Fernandez R, Miller A, Pong S, Powers BW, Pupo-Wiss A, Stanhope ME, Walsh PJ, Wiwatpanit T, and Christie AE. Three members of a peptide family are differentially distributed and elicit differential state-dependent responses in a pattern generator-effector system. *J Neurophysiol* 119: 1767-1781, 2018.

Dickinson PS, Dickinson ES, Oleisky ER, Rivera CD, Stanhope ME, Stemmler EA, Hull JJ, and Christie AE. AMGSEFLamide, a member of a broadly conserved peptide family, modulates multiple neural networks in *Homarus americanus*. *J Exp Biol* 222: 2019a.

Dickinson PS, Hull JJ, Miller A, Oleisky ER, and Christie AE. To what extent may peptide receptor gene diversity/complement contribute to functional flexibility in a simple pattern-generating neural network? *Comparative biochemistry and physiology Part D, Genomics & proteomics* 30: 262-282, 2019b.

Dickinson PS, Qu X, and Stanhope ME. Neuropeptide modulation of pattern-generating systems in crustaceans: comparative studies and approaches. *Current opinion in neurobiology* 41: 149-157, 2016.

Dickinson PS, Sreekrishnan A, Kwiatkowski MA, and Christie AE. Distinct or shared actions of peptide family isoforms: I. Peptide-specific actions of pyrokinins in the lobster cardiac neuromuscular system. *J Exp Biol* 218: 2892-2904, 2015.

Dickinson PS, Stevens JS, Rus S, Brennan HR, Goiney CC, Smith CM, Li L, Towle DW, and Christie AE. Identification and cardiotropic actions of sulfakinin peptides in the American lobster *Homarus americanus*. *Journal of Experimental Biology* 210: 2278-2289, 2007.

Edgar RC. MUSCLE: a multiple sequence alignment method with reduced time and space complexity. *BMC bioinformatics* 5: 113, 2004.

Egerod K, Reynisson E, Hauser F, Cazzamali G, Williamson M, and Grimmelikhuijzen CJ. Molecular cloning and functional expression of the first two specific insect myosuppressin receptors. *Proceedings of the National Academy of Sciences of the United States of America* 100: 9808-9813, 2003.

El-Gebali S, Mistry J, Bateman A, Eddy SR, Luciani A, Potter SC, Qureshi M, Richardson LJ, Salazar GA, Smart A, Sonnhammer ELL, Hirsh L, Paladin L, Piovesan D, Tosatto SCE, and Finn RD. The Pfam protein families database in 2019. *Nucleic Acids Res* 47: D427-d432, 2019.

Elia AJ, Tebrugge VA, and Orchard I. The pulsatile appearance of FMRFamide-related peptides in the haemolymph and loss of FMRFamide-like immunoreactivity from neurohaemal areas of *Rhodnius prolixus* following a blood meal. *J Insect Physiol* 39: 459-469, 1993.

Elson RC, and Selverston AI. Evidence for a persistent Na+ conductance in neurons of the gastric mill rhythm generator of spiny lobsters. *Journal of Experimental Biology* 200: 1795-1807, 1997.

Fastner S, Predel R, Kahnt J, Schachtner J, and Wegener C. A simple purification protocol for the detection of peptide hormones in the hemolymph of individual insects by matrix-assisted laser desorption/ionization time-of-flight mass spectrometry. *Rapid communications in mass spectrometry : RCM* 21: 23-28, 2007.

Ferre F, and Clote P. DiANNA: a web server for disulfide connectivity prediction. *Nucleic Acids Res* 33: W230-232, 2005.

Fort TJ, Brezina V, and Miller MW. Modulation of an integrated central pattern generator-effector system: dopaminergic regulation of cardiac activity in the blue crab *Callinectes sapidus*. *J Neurophysiol* 92: 3455-3470, 2004.

Fort TJ, Brezina V, and Miller MW. Regulation of the crab heartbeat by FMRFamide-like peptides: multiple interacting effects on center and periphery. *J Neurophysiol* 98: 2887-2902, 2007a.

Fort TJ, Garcia-Crescioni K, Agricola HJ, Brezina V, and Miller MW. Regulation of the crab heartbeat by crustacean cardioactive peptide (CCAP): central and peripheral actions. *J Neurophysiol* 97: 3407-3420, 2007b.

Garcia VJ, Daur N, Temporal S, Schulz DJ, and Bucher D. Neuropeptide receptor transcript expression levels and magnitude of ionic current responses show cell type-specific differences in a small motor circuit. *The Journal of neuroscience : the official journal of the Society for Neuroscience* 35: 6786-6800, 2015.

Grashow R, Brookings T, and Marder E. Compensation for variable intrinsic neuronal excitability by circuit-synaptic interactions. *The Journal of Neuroscience* 30: 9145-9156, 2010.

Gunay C, Edgerton JR, and Jaeger D. Channel density distributions explain spiking variability in the globus pallidus: a combined physiology and computer simulation database approach. *The Journal of neuroscience : the official journal of the Society for Neuroscience* 28: 7476-7491, 2008.

Guo W, Jung WE, Marionneau C, Aimond F, Xu H, Yamada KA, Schwarz TL, Demolombe S, and Nerbonne JM. Targeted deletion of Kv4.2 eliminates $I_{to,f}$ and results in electrical and molecular remodeling, with no evidence of ventricular hypertrophy or myocardial dysfunction. *Circulation Research* 97: 1342-1350, 2005.

Hartline DK. Impulse identification and axon mapping of the nine neurons in the cardiac ganglion of the lobster *Homarus americanus*. *J Exp Biol* 47: 327-340, 1967.

Hauser F, Williamson M, Cazzamali G, and Grimmelikhuijzen CJP. Identifying neuropeptide and protein hormone receptors in *Drosophila melanogaster* by exploiting genomic data. *Briefings in Functional Genomics* 4: 321-330, 2006.

Johnson EC, Bohn LM, Barak LS, Birse RT, Nässel DR, Caron MG, and Taghert PH. Identification of Drosophila neuropeptide receptors by G protein-coupled receptors-β-arrestin2 interactions. *J Biol Chem* 278: 52172-52178, 2003.

Jones DT, Taylor WR, and Thornton JM. The rapid generation of mutation data matrices from protein sequences. *Comput Appl Biosci* 8: 275–282, 1992.

Kang BJ, Okutsu T, Tsutsui N, Shinji J, Bae SH, and Wilder MN. Dynamics of vitellogenin and vitellogenesis-inhibiting hormone levels in adult and subadult whiteleg

shrimp, *Litopenaeus vannamei*: relation to molting and eyestalk ablation. *Biology of reproduction* 90: 12, 2014.

Katoh K, and Standley DM. MAFFT multiple sequence alignment software version 7: improvements in performance and usability. *Molecular biology and evolution* 30: 772-780, 2013.

Katz PS. Intrinsic and extrinsic neuromodulation of motor circuits. *Current opinion in neurobiology* 5: 799-808, 1995.

Katz PS, and Frost WN. Intrinsic neuromodulation: altering neuronal circuits from within. *Trends in neurosciences* 19: 54-61, 1996.

Kearse M, Moir R, Wilson A, Stones-Havas S, Cheung M, Sturrock S, Buxton S, Cooper A, Markowitz S, Duran C, Thierer T, Ashton B, Meintjes P, and Drummond A. Geneious Basic: an integrated and extendable desktop software platform for the organization and analysis of sequence data. *Bioinformatics (Oxford, England)* 28: 1647-1649, 2012.

Kobierski LA, Beltz BS, Trimmer BA, and Kravitz EA. FMRFamidelike peptides of *Homarus americanus*: distribution, immunocytochemical mapping, and ultrastructural localization in terminal varicosities. *The Journal of comparative neurology* 266: 1-15, 1987.

Kumar S, Stecher G, Li M, Knyaz C, and Tamura K. MEGA X: Molecular Evolutionary Genetics Analysis across computing platforms. *Molecular biology and evolution* 35: 1547-1549, 2018.

Lane BJ, Samarth P, Ransdell JL, Nair SS, and Schulz DJ. Synergistic plasticity of intrinsic conductance and electrical coupling restores synchrony in an intact motor network. *eLife* 5: 2016.

Le SQ, and Gascuel O. An improved general amino acid replacement matrix. *Molecular biology and evolution* 25: 1307-1320, 2008.

MacLean JN, Zhang Y, Goeritz ML, Casey R, Oliva R, Guckenheimer J, and Harris-Warrick RM. Activity-independent coregulation of IA and Ih in rhythmically active neurons. *J Neurophysiol* 94: 3601-3617, 2005.

MacLean JN, Zhang Y, Johnson BR, and Harris-Warrick RM. Activity-independent homeostasis in rhythmically active neurons. *Neuron* 37: 109-120, 2003.

Marder E. Variability, compensation, and modulation in neurons and circuits. *Proceedings of the National Academy of Sciences of the United States of America* 108 Suppl 3: 15542-15548, 2011.

Marder E, and Calabrese RL. Principles of rhythmic motor pattern generation. *Physiological reviews* 76: 687-717, 1996.

Marder E, and Goaillard JM. Variability, compensation and homeostasis in neuron and network function. *Nature reviews Neuroscience* 7: 563-574, 2006.

Mayeri E. Functional organization of the cardiac ganglion of the lobster, *Homarus americanus*. *The Journal of general physiology* 62: 448-472, 1973.

Messinger DI, Kutz KK, Le T, Verley DR, Hsu Y-WA, Ngo CT, Cain SD, Birmingham JT, Li L, and Christie AE. Identification and characterization of a tachykinin-containing neuroendocrine organ in the commissural ganglion of the crab *Cancer productus*. *Journal of Experimental Biology* 208: 3303-3319, 2005.

Miller MW, and Sullivan RE. Some effects of proctolin on the cardiac ganglion of the Maine Lobster, *Homarus americanus* (Milne Edwards). *Journal of neurobiology* 12: 629-639, 1981.

Monigatti F, Gasteiger E, Bairoch A, and Jung E. The Sulfinator: predicting tyrosine sulfation sites in protein sequences. *Bioinformatics (Oxford, England)* 18: 769-770, 2002.

Morris C, and Lecar H. Voltage oscillations in the barnacle giant muscle fiber. *Biophys J* 35: 193-213, 1981.

Motulsky HJ, and Brown RE. Detecting outliers when fitting data with nonlinear regression - a new method based on robust nonlinear regression and the false discovery rate. *BMC bioinformatics* 7: 123, 2006.

Nagy F, Dickinson PS, and Moulins M. Rhythmical synaptic control of axonal conduction in a lobster motor neuron. *J Neurophysiol* 45: 1109-1124, 1981.

Nerbonne JM, Gerber BR, Norris A, and Burkhalter A. Electrical remodelling maintains firing properties in cortical pyramidal neurons lacking KCND2-encoded A-type K+ currents. *The Journal of physiology* 586: 1565-1579, 2008.

Northcutt AJ, Lett KM, Garcia VB, Diester CM, Lane BJ, Marder E, and Schulz DJ. Deep sequencing of transcriptomes from the nervous systems of two decapod crustaceans to characterize genes important for neural circuit function and modulation. *BMC genomics* 17: 868, 2016.

Olypher AV, and Calabrese RL. Using constraints on neuronal activity to reveal compensatory changes in neuronal parameters. *Journal of Neurophysiology* 98: 3749-3758, 2007.

Price DA, Cobb CG, Doble KE, Kline JK, and Greenberg MJ. Evidence for a novel FMRFamide-related heptapeptide in the pulmonate snail *Siphonaria pectinata*. *Peptides* 8: 533-538, 1987.

Ramirez JM, Tryba AK, and Pena F. Pacemaker neurons and neuronal networks: an integrative view. *Current opinion in neurobiology* 14: 665-674, 2004.

Ransdell JL, Nair SS, and Schulz DJ. Rapid homeostatic plasticity of intrinsic excitability in a central pattern generator network stabilizes functional neural network output. *The Journal of Neuroscience* 32: 9649-9658, 2012.

Ransdell JL, Temporal S, West NL, Leyrer ML, and Schulz DJ. Characterization of inward currents and channels underlying burst activity in motoneurons of crab cardiac ganglion. *J Neurophysiol* 110: 42-54, 2013.

Robb S, and Evans PD. FMRFamide-like peptides in the locust: distribution, partial characterization and bioactivity. *J Exp Biol* 149: 335-360, 1990.

Rzhetsky A, and Nei M. A simple method for estimating and testing minimum-evolution trees. *Molecular biology and evolution* 9: 945-945, 1992.

Saitou N, and Nei M. The neighbor-joining method: a new method for reconstructing phylogenetic trees. *Molecular biology and evolution* 4: 406-425, 1987.

Schulz DJ, Goaillard J-M, and Marder E. Variable channel expression in identified single and electrically coupled neurons in different animals. *Nature neuroscience* 9: 356-362, 2006.

Stemmler EA, Cashman CR, Messinger DI, Gardner NP, Dickinson PS, and Christie AE. High-mass-resolution direct-tissue MALDI-FTMS reveals broad conservation of three neuropeptides (APSGFLGMRamide, GYRKPPFNGSIFamide and pQDLDHVFLRFamide) across members of seven decapod crustaean infraorders. *Peptides* 28: 2104-2115, 2007.

Stevens JS, Cashman CR, Smith CM, Beale KM, Towle DW, Christie AE, and Dickinson PS. The peptide hormone pQDLDHVFLRFamide (crustacean myosuppressin) modulates the *Homarus americanus* cardiac neuromuscular system at multiple sites. *Journal of Experimental Biology* 212: 3961-3976, 2009.

Sullivan RE, and Miller MW. Dual effects of proctolin on the rhythmic burst activity of the cardiac ganglion. *Journal of neurobiology* 15: 173-196, 1984.

Swensen AM, and Bean BP. Robustness of burst firing in dissociated purkinje neurons with acute or long-term reductions in sodium conductance. *The Journal of neuroscience : the official journal of the Society for Neuroscience* 25: 3509-3520, 2005.

Tazaki K, and Cooke IM. Characterization of Ca current underlying burst formation in lobster cardiac ganglion motorneurons. *J Neurophysiol* 63: 370-384, 1990.

Tazaki K, and Cooke IM. Currents under voltage clamp of burst-forming neurons of the cardiac ganglion of the lobster (*Homarus americanus*). *J Neurophysiol* 56: 1739-1762, 1986.

Tazaki K, and Cooke IM. Separation of neuronal sites of driver potential and impulse generation by ligaturing in the cardiac ganglion of the lobster *Homarus americanus*.

Journal of Comparative Physiology A Sensory Neural and Behavioral Physiology 151: 329-346, 1983.

Thoby-Brisson M, and Simmers J. Long-term neuromodulatory regulation of a motor pattern–generating network: maintenance of synaptic efficacy and oscillatory properties. *Journal of Neurophysiology* 88: 2942-2953, 2002.

Thoby-Brisson M, and Simmers J. Neuromodulatory inputs maintain expression of a lobster motor pattern-generating network in a modulation-dependent state: evidence from long-term decentralization in vitro. *The Journal of neuroscience : the official journal of the Society for Neuroscience* 18: 2212-2225, 1998.

Thurmond J, Goodman JL, Strelets VB, Attrill H, Gramates LS, Marygold SJ, Matthews BB, Millburn G, Antonazzo G, Trovisco V, Kaufman TC, and Calvi BR. FlyBase 2.0: the next generation. *Nucleic Acids Res* 47: D759-d765, 2019.

Tsirigos KD, Peters C, Shu N, Käll L, and Elofsson A. The TOPCONS web server for consensus prediction of membrane protein topology and signal peptides. *Nucleic Acids Res* 43: W401–W407, 2015.

Turrigiano G, LeMasson G, and Marder E. Selective regulation of current densities underlies spontaneous changes in the activity of cultured neurons. *The Journal of Neuroscience* 15: 3640-3652, 1995.

Wilhelm JC, Rich MM, and Wenner P. Compensatory changes in cellular excitability, not synaptic scaling, contribute to homeostatic recovery of embryonic network activity. *Proceedings of the National Academy of Sciences* 106: 6760-6765, 2009.

Williams AH, Kwiatkowski MA, Mortimer AL, Marder E, Zeeman ML, and Dickinson PS. Animal-to-animal variability in the phasing of the crustacean cardiac motor pattern: an experimental and computational analysis. *J Neurophysiol* 109: 2451-2465, 2013.

Wurch T, Lestienne F, and Pauwels PJ. A modified overlap extension PCR method to create chimeric genes in the absence of restriction enzymes. *Biotechnology Techniques* 12: 653-657, 1998.

Zitnan D, Ross LS, Zitnanova I, Hermesman JL, Gill SS, and Adams ME. Steroid induction of a peptide hormone gene leads to orchestration of a defined behavioral sequence. *Neuron* 23: 523-535, 1999.

FIGURE LEGENDS

Figure 1. Schematic diagram of the cardiac ganglion (CG) of the American lobster, *Homarus americanus*. A) Organization of the cardiac ganglion with ligature and petroleum jelly well placement. Four small premotor neurons located in the posterior trunk of the cardiac ganglion are electrically and chemically coupled to the five large motor neurons, which are located in the anterior portion of the cardiac ganglion. All nine neurons are electrically and chemically coupled. Green indicates motor neurons and purple indicates premotor neurons. Green and purple ovals indicate the location of recording sites. Site of the ligature is indicated by thread loop. **B)** Diagram of physiologically determined anatomy (Hartline 1967) of the trigger-zone locations within the trunk of the CG.

Figure 2. Baseline firing pattern differs in the intact and ligatured cardiac ganglion. A) In the intact CG, the premotor (purple) and motor (green) neuron bursts are in-phase, with the premotor bursts beginning just before motor neuron bursting. In most preparations (19/25), only motor neuron bursting was captured by the well on the anterolateral nerve (*aln)*, while the well on the trunk captured both premotor and motor bursting activity. **B)** When ligatured, the premotor and motor bursts exhibited bursting patterns independent of one another. The baseline firing frequency of the motor neurons was slower, with longer baseline burst durations in the premotor firing pattern.

Figure 3. Baseline burst characteristics of the intact and ligatured cardiac ganglion. A) The burst duration of the premotor neurons (PN) did not change with the ligature (0.63 s ± 0.19 s vs. 0.6 s ± 0.2 s), but tightening elicited a significant decrease in burst duration of the motor neurons (MN; 0.4 s ± 0.2 s vs. 0.24 s ± 0.07 s). Inset: a single burst at a higher recording speed shows that the burst of small premotor neuron spikes (purple) starts before and ends after the burst of larger motor neuron spikes (green). **B)** The frequency of bursts in the premotor neurons did not change with the ligature (0.40 Hz ± 0.11 Hz vs. 0.47 Hz ± 0.12 Hz), but ligaturing the CG elicited a significant decrease in motor neuron burst frequency (0.32 Hz ± 0.09 Hz vs. 0.40 Hz ± 0.11 Hz). * Indicates significant change with tightening of the ligature (one-way ANOVAs with post-hoc

Tukey tests. Burst duration: intact PN vs. MN, $p < 0.0001$; intact vs. ligatured MN, $p = 0.0042$, ligatured PN vs. MN, $p < 0.0001$, $n = 18$. Burst frequency: intact vs. ligatured MN, $p = 0.0338$; ligatured PN vs. MN, $p = 0.0005$, $n = 18$). Error bars indicate SD.

Figure 4. The bursting activity of the intact and ligatured cardiac ganglion in response to myosuppressin application. At both 10^{-7} M and 10^{-6} M, myosuppressin application qualitatively altered the bursting pattern of the intact and ligatured premotor and motor neurons. In the ligatured CG, myosuppressin differentially altered the bursting pattern of the premotor and motor neurons. All extracellular traces are from the same individual.

Figure 5. Myosuppressin altered the burst characteristics of the intact and ligatured ganglion. Myosuppressin elicited changes in burst frequency **(A, D)**, interburst interval **(B, E)**, and burst duration **(C, F)** at 10^{-7} M (A-C, $n = 8$) and 10^{-6} M (D-F, $n = 10$) in the intact and ligatured CG. The ROUT method was used to eliminate outliers.
* represents significant change from baseline (One sample t-tests: burst frequency, 10^{-7} M (PN and MN, intact, $p = 0.0058$; MN ligatured, $p < 0.0001$), interburst interval, 10^{-7} M (PN intact, $p = 0.0332$; MN intact, $p = 0.0365$; MN ligatured, $p = 0.0018$), burst frequency, 10^{-6} M (PN and MN, intact and ligatured, $p < 0.0001$), burst duration, 10^{-6} M (PN intact, $p = 0.0030$; MN intact, $p = 0.0014$; PN ligatured, $p < 0.0001$), interburst interval, 10^{-6} M (PN intact, $p = 0.0022$; MN intact, $p = 0.0021$; PN ligatured, $p = 0.0033$; MN ligatured, $p = 0.0075$)). Error bars indicate SD. Changes in both neuronal types were larger in magnitude in response to 10^{-6}M myosuppressin than in response to 10^{-7}M myosuppressin (Mann-Whitney tests. Burst frequency: PN and MN, $p = 0.0044$. Burst duration: PN, $p = 0.0031$; MN, $p < 0.0001$. Interburst interval: PN and MN, $p = 0.0021$).

add space

add space

Figure 6. The response to myosuppressin in the ligatured premotor neurons has a later onset than in the motor neurons. The bursting activity of the premotor (purple) and motor (green) neurons in a ligatured CG preparation before myosuppressin

application (saline) and during the final 200 s of the 10-minute 10^{-6} M myosuppressin application. The burst frequency of the ligatured motor neurons decreased continuously during peptide application. The large magnitude increases in burst duration and decreases in burst frequency in the premotor neurons appeared later during peptide application, as the shorter bursts of the ligatured premotor neurons were overtaken by a pattern of longer bursts at lower frequency.

Figure 7. MAFFT alignment of select putative *Homarus americanus* myosuppressin receptors. All proteins identified and shown in this figure are full-length sequences except for MSR-IIIa, which is a carboxyl-terminal partial protein. The relative position of predicted transmembrane domains are indicated by blue boxes. The 13 amino acid amino-terminal extension that distinguishes MSR-II-v1 from MSR-II-v2 (not shown) is highlighted in yellow. The single amino acid substitutions that distinguish MSR-III "a" and "b" morphs (asparagine in a IIIa vs. threonine in IIIb [not shown]) and MSR-IV "a" and "b" morphs (methionine in IVa vs. valine in IVb [not shown]) are colored red. Receptor abbreviations: MSR-I, myosuppressin receptor I; MSR-II-v1, myosuppressin receptor II variant 1; MSR-IIIa, myosuppressin receptor IIIa; MSR-IVa, myosuppressin receptor IVa; MSR-V, myosuppressin receptor V.

delete "a"?

Figure 8. Maximum likelihood tree depicting phylogenetic relationships among putative *Homarus americanus* myosuppressin receptors and *Drosophila melanogaster* peptide receptors. The tree with the highest log likelihood is shown and the percentage of trees in which the associated taxa clustered together (1000 replicates) is shown next to the branches. The tree is drawn to scale, with branch lengths measured in the number of substitutions per site. Drome MSRs functionally characterized as myosuppressin receptors (Egerod et al., 2003; Johnson et al., 2003) are indicated in italics.

Figure 9. PCR confirmed the differential expression of myosuppressin and putative myosuppressin receptors (MSRs) in the premotor and motor neurons of the *Homarus americanus* CG. RT-PCR based amplification of the myosuppressin

preprohormone **(A)** and myosuppressin receptors **(B)** from three biological replicates of premotor and motor neuron cDNAs. Brain (Br) and eyestalk ganglia (EG) were included as positive controls for MSR amplification. NT corresponds to the no template control. To confirm cDNA quality, a 500-bp fragment of *Homarus* GAPDH was amplified. Representative image corresponds to PCR products electrophoresed on 1.5% agarose gels stained with SYBR Safe.

Table 1. Oligonucleotide primers used.

Primer	Sequence (5' → 3')
Cloning / Expression profiling	
HaMS start F	ATGGTGTTCCGCAGCTG
HaMS stop R	TTATTGCTGGGATCGTCCGA
Cloning	
HaMSR-I start F	ATGGAGCAGGTGGAGGC
HaMSR-I stop R	TCAGACATGTGTGATACATGTG
HaMSR-II start F	ATGTTTAGTGTTAACTTTAGCGAG
HaMSR-II stop R	TCAGACATGTGTGATGCAG
HaMSR-III 350	CCGTGATCTGCAACATCC
HaMSR-III stop R	TCACCAAACTCTGGTGTGTTCC
HaMSR-IV start F	ATGATGACTGCGGGGAGC
HaMSR-IV 755 R	TGTAGCAGGCCATTCGAT
HaMSR-IV 252 F	CTTGGCGCTGATGATCTG
HaMSR-IV stop R	TTAGAGCTGGGTAGAAACTGTC
HaMSR-V start F	ATGGAGCGGTCCCTGC
HaMSR-V stop R	TCATATCTTAGTGTTAAGAACTTTGC
Expression profiling	
HaMSR-I 653 F	ACTTCACCATCAGCACGA
HaMSR-I 1173 R	GCGGATAGATAGCACCGA
HaMSR-II 179 F	CCACCACACAAGACTCCT
HaMSR-II 682 R	GGATGTTGCAGATGACGG
HaMSR-III 350 F	CCGTGATCTGCAACATCC
HaMSR-III 816 R	CAGCAGGAAGTTGATGGC
HaMSR-IV 252 F	CTTGGCGCTGATGATCTG
HaMSR-IV 755 R	TGTAGCAGGCCATTCGAT
HaMSR-V 695 F	TGTCCAACGATGACGGAT
HaMSR-V 1229 R	TTGATGAGCGCCAACAAG
HaGAPDH 96 F	TCGGTCGTCTTGTCCTTC
HaGAPDH 599 R	CAGTGACGGCATGAACAG

Ha, *Homarus americanus*; myo, myosuppressin; MS, myosuppressin; MSR, myosuppressin receptor; GAPDH, glyceraldehyde-3-phosphate dehydrogenase; F, forward; R, reverse

Table 2. *In silico* detection of putative myosuppressin receptors in the nervous system of *Homarus americanus*

Assembly	Receptor				
	MSR-I	MSR-II	MSR-III	MSR-IV	MSR-V
Mixed	+	+	+	+	+
Br	+	+	+[1]	+	+
EG	+	+	+	+	+
CG	–	+[2]	+	+	–

Assembly abbreviations: Mixed, mixed nervous system; Br, brain-specific; EG, eyestalk ganglia-specific; CG, cardiac ganglion specific.

hyphenate

Receptor abbreviations (reference for first identification): MSR-I, myosuppressin receptor I (Christie et al., 2015); MSR-II, myosuppressin receptor II (this study); MSR-III, myosuppressin receptor III (this study); MSR-IV, myosuppressin receptor IV (this study); MSR-V, myosuppressin receptor V (this study).

[1]A 131 amino acid internal fragment that differs from the corresponding portion of MSR-III at five positions (three conservative and two non-conservative substitutions) was predicted from the brain-specific assembly. Whether this partial protein represents a variant of MSR-III or an additional myosuppressin receptor (MSR-VI) remains to be determined.

[2]Two splice variants of MSR-II appear to be expressed in the CG.

Table 3. Matrix of percent amino acid identity/similarity* between select putative *Homarus americanus* myosuppressin receptor proteins

	MSR-I	MSR-II-v1	MSR-IIIa	MSR-IVa	MSR-V
MSR-I	–	73/87	85/95	37/69	32/65
MSR-II-v1		–	86/96	37/69	35/68
MSR-IIIa			–	45/74	36/68
MSR-IVa				–	35/68
MSR-V					–

*Percent identity/similarity between MSR-IIIa and all other receptors was calculated using only the regions of overlap, as MSR-IIIa is a C-terminal partial protein. Calculations are based on the proteins deduced from the transcriptomic data presented in this paper.

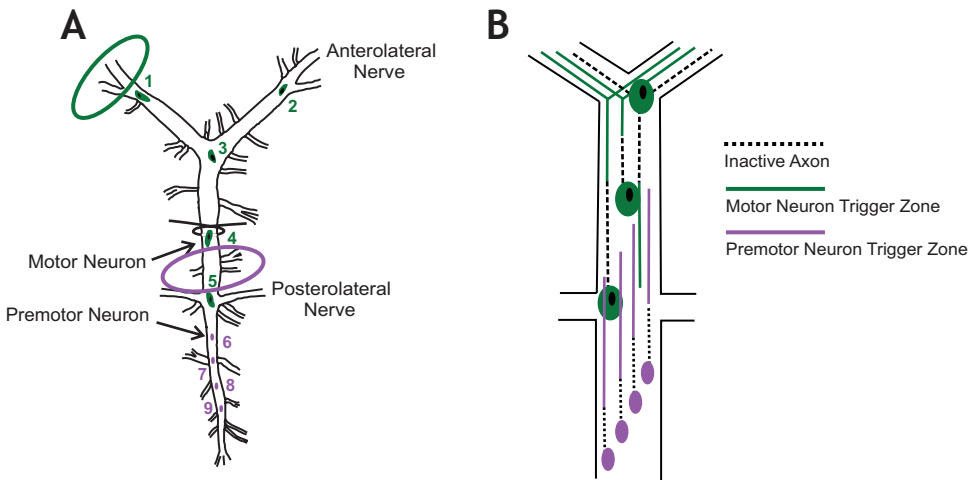
A
Anterolateral Nerve
1
2
3
4
Motor Neuron
5
Posterolateral Nerve
Premotor Neuron
6
7
8
9
B
Inactive Axon
Motor Neuron Trigger Zone
Premotor Neuron Trigger Zone

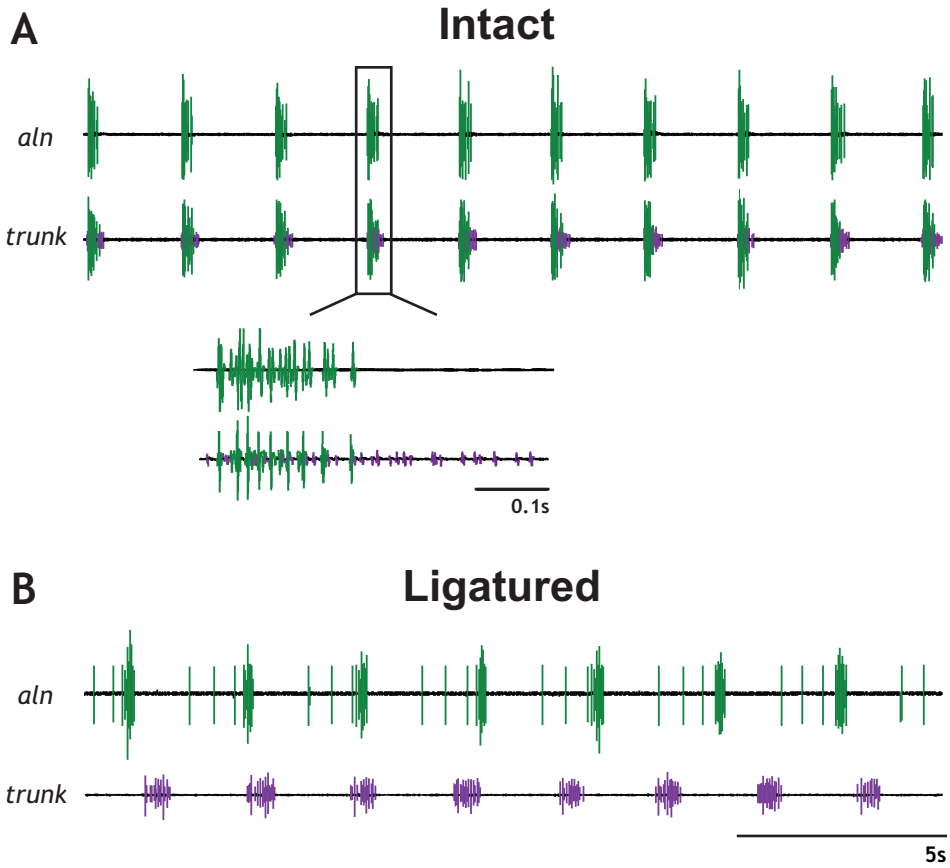
A
Intact
aln
trunk
0.1s
B
Ligatured
aln
trunk
5s

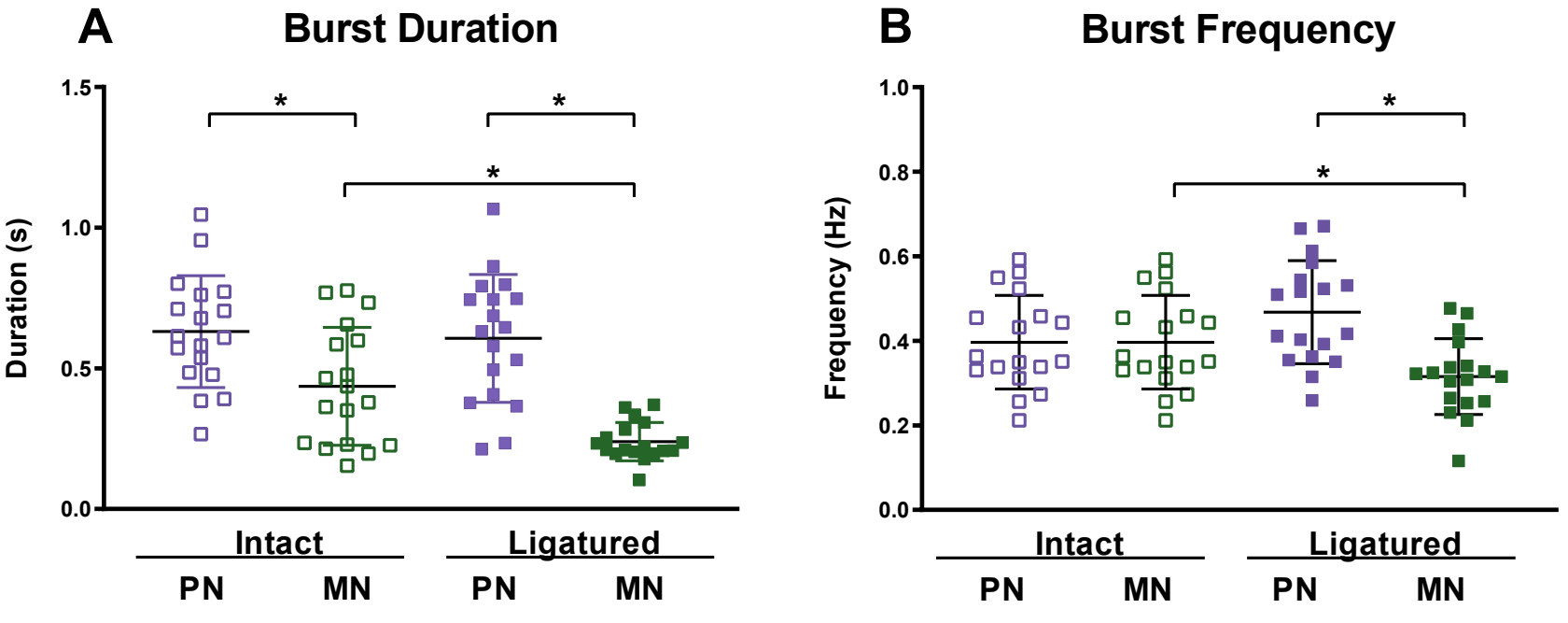
A
Burst Duration
Duration (s)
1.5
1.0
0.5
0.0
*
*
*
Intact
Ligatured
PN
MN
PN
MN
B
Burst Frequency
Frequency (Hz)
1.0
0.8
0.6
0.4
0.2
0.0
*
*
Intact
Ligatured
PN
MN
PN
MN

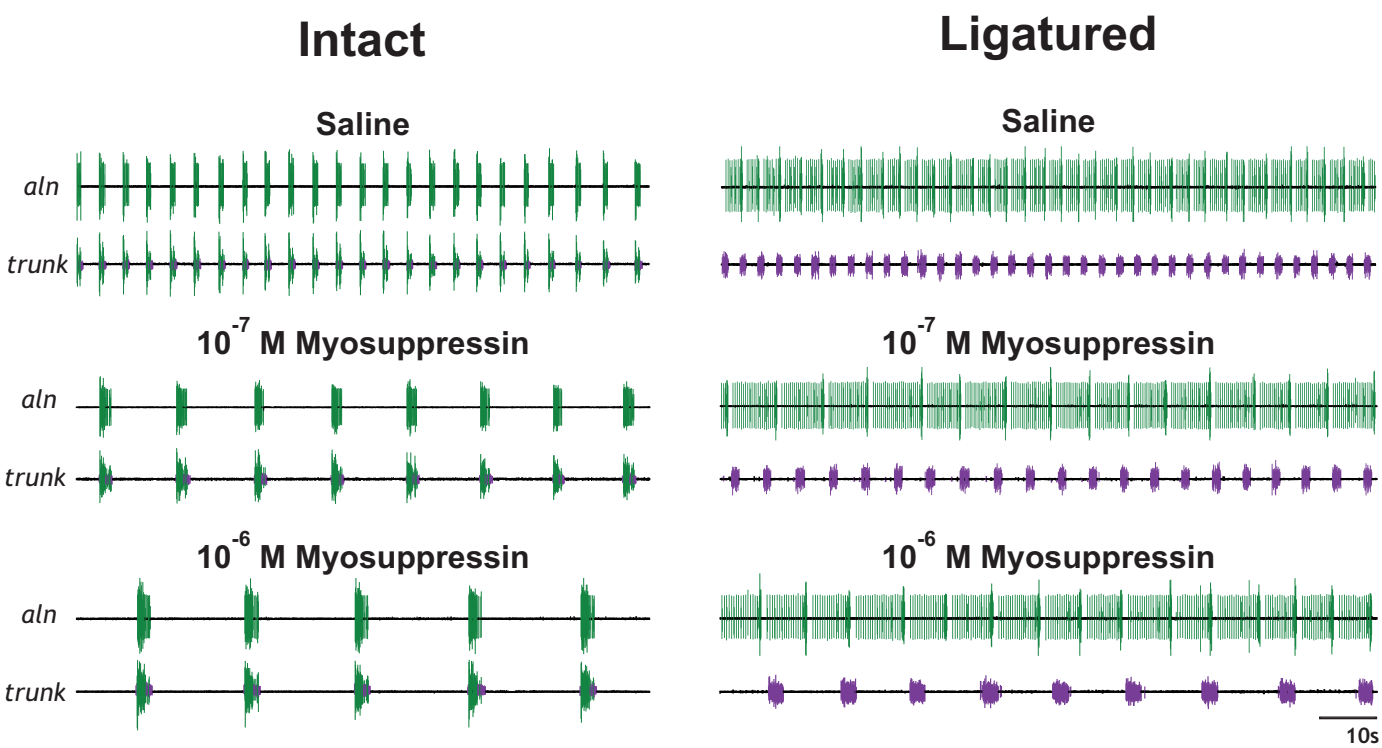
Intact
Ligatured
Saline
aln
trunk
10-7 M Myosuppressin
10-6 M Myosuppressin
10s

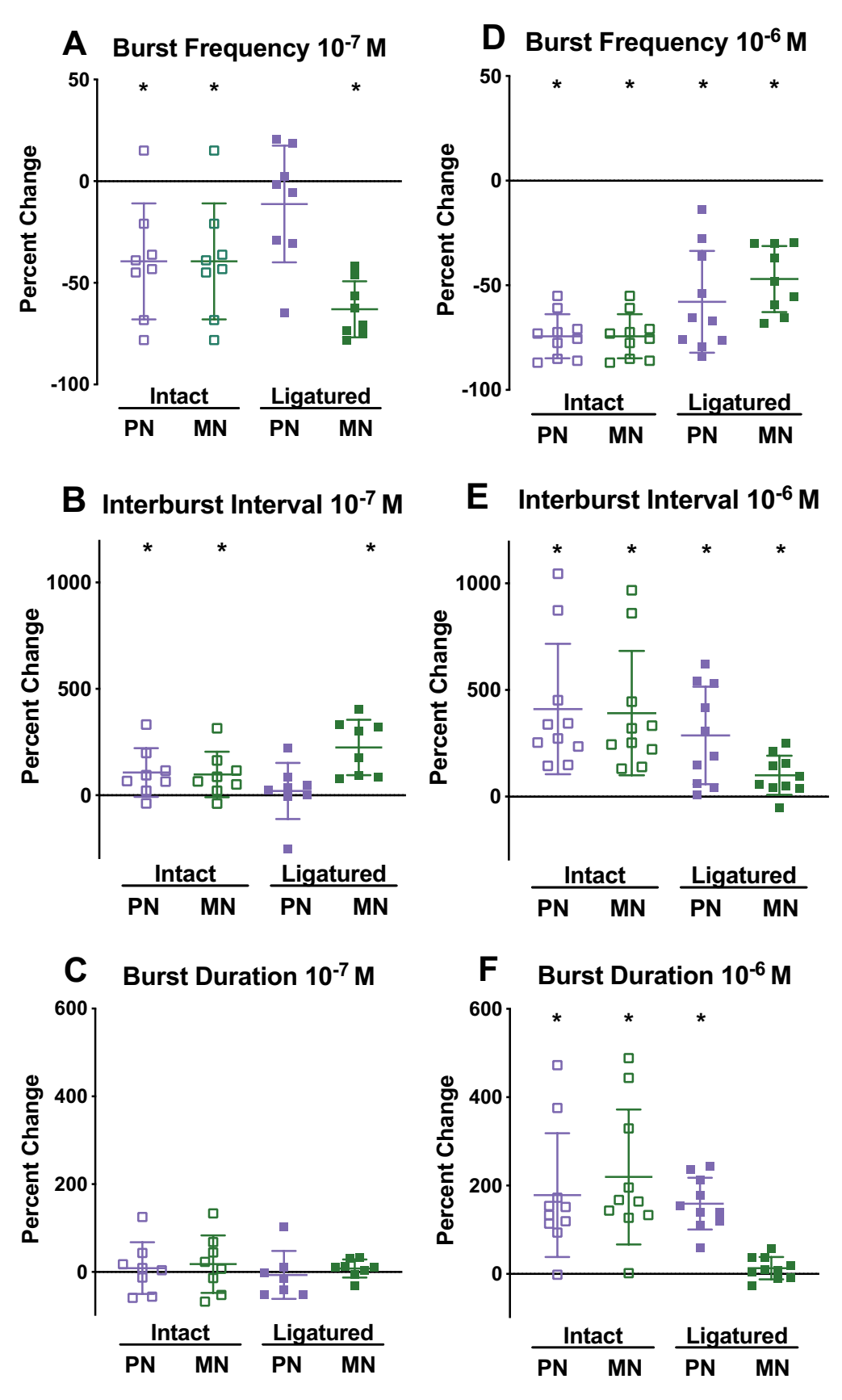
A
Burst Frequency 10-7 M
Percent Change
50
0
-50
-100
*
*
*
Intact
Ligatured
PN
MN
PN
MN
D
Burst Frequency 10-6 M
B
Interburst Interval 10-7 M
1000
500
E
Interburst Interval 10-6 M
C
Burst Duration 10-7 M
600
400
200
F
Burst Duration 10-6 M

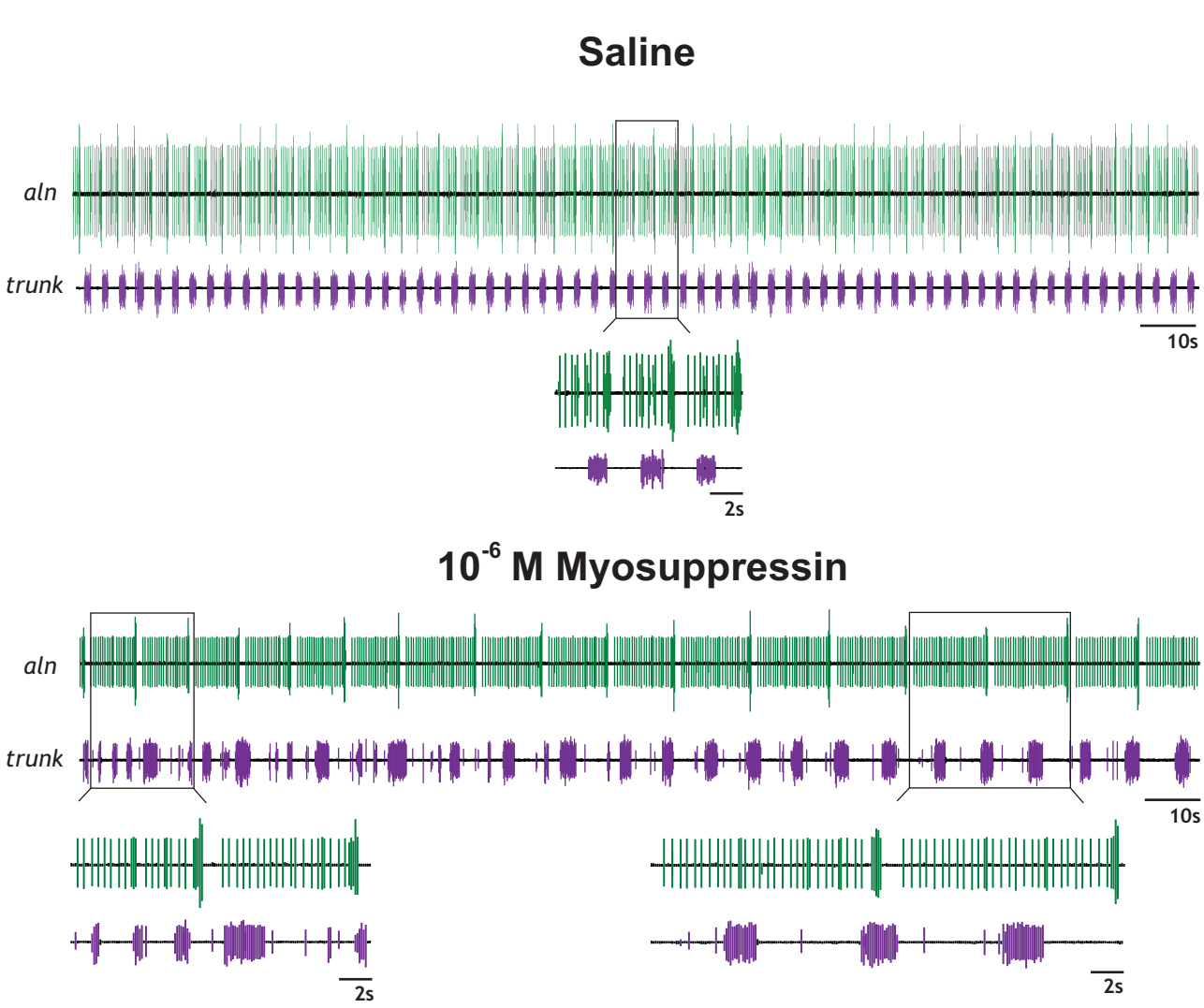
Saline
aln
trunk
10s
2s
10-6 M Myosuppressin
aln
trunk
10s
2s
2s

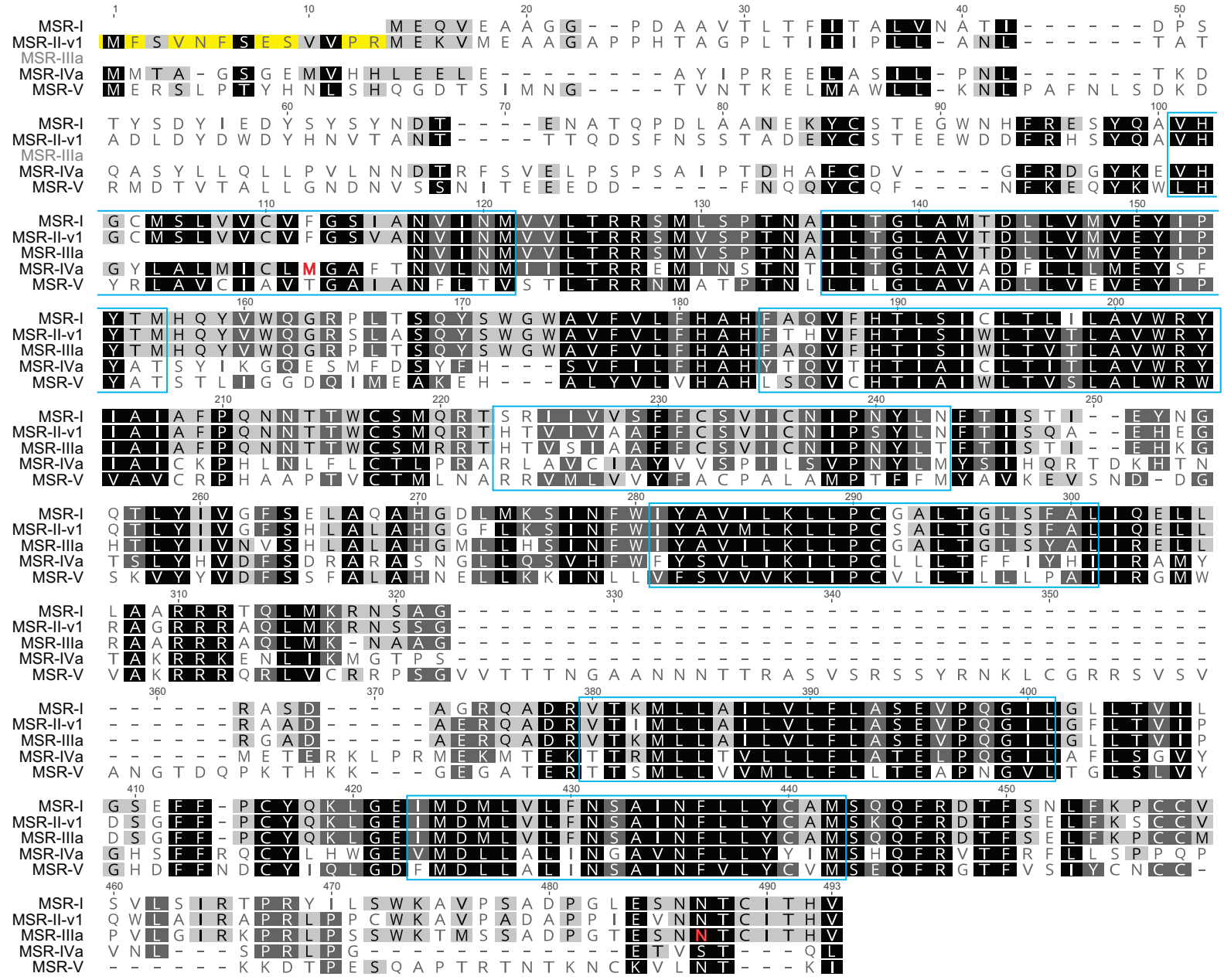
MSR-I
MSR-II-v1
MSR-IIIa
MSR-IVa
MSR-V

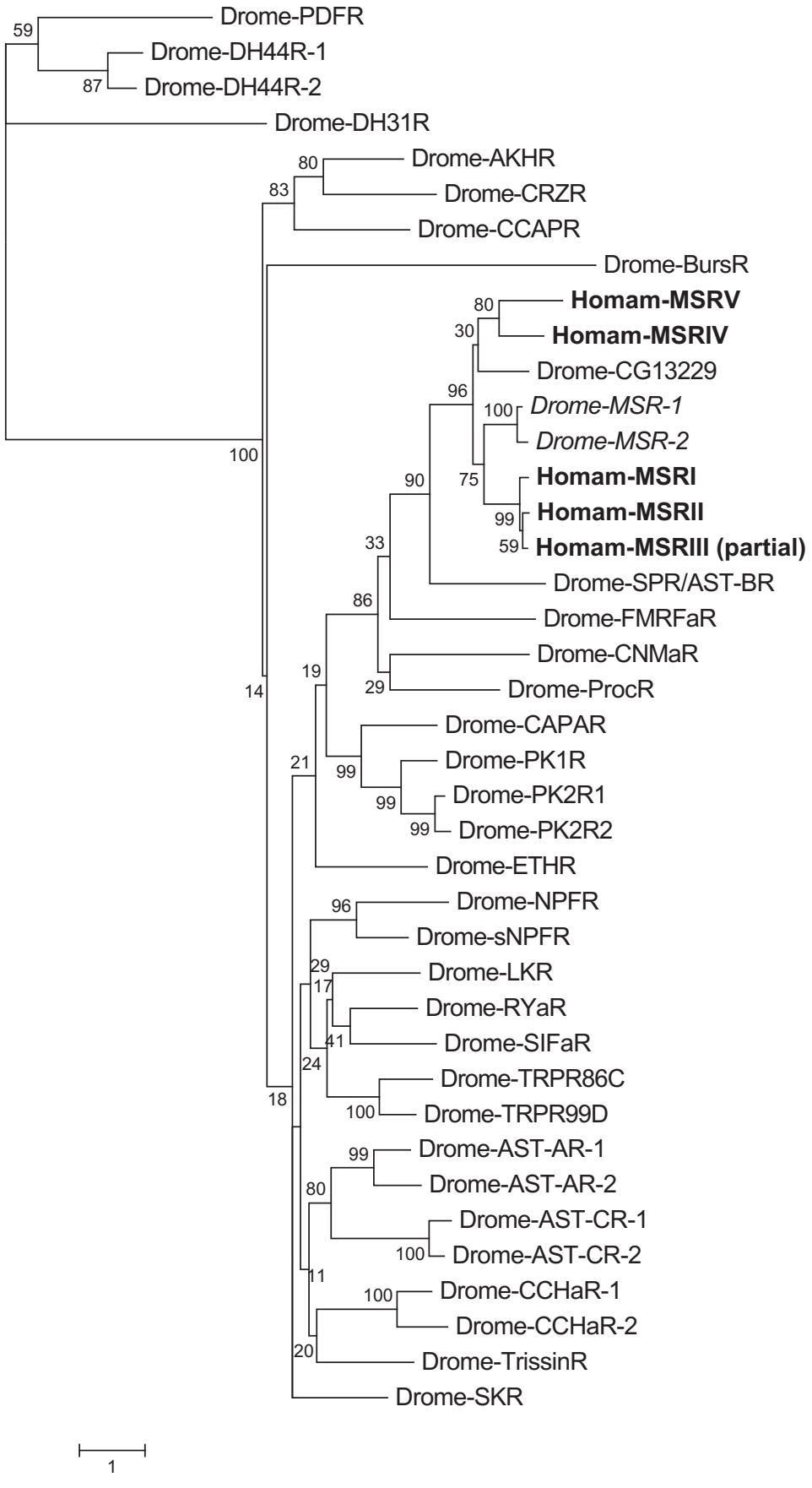
Drome-PDFR
59
Drome-DH44R-1
87
Drome-DH44R-2
Drome-DH31R
80
Drome-AKHR
83
Drome-CRZR
Drome-CCAPR
Drome-BursR
80
Homam-MSRV
30
Homam-MSRIV
Drome-CG13229
96
100
Drome-MSR-1
Drome-MSR-2
100
90
75
Homam-MSRI
99
Homam-MSRII
59
Homam-MSRIII (partial)
33
Drome-SPR/AST-BR
86
Drome-FMRFaR
Drome-CNMaR
19
29
Drome-ProcR
14
Drome-CAPAR
21
Drome-PK1R
99
99
Drome-PK2R1
99
Drome-PK2R2
Drome-ETHR
96
Drome-NPFR
Drome-sNPFR
29
Drome-LKR
17
Drome-RYaR
41
Drome-SIFaR
24
Drome-TRPR86C
18
100
Drome-TRPR99D
99
Drome-AST-AR-1
Drome-AST-AR-2
80
Drome-AST-CR-1
100
Drome-AST-CR-2
11
100
Drome-CCHaR-1
Drome-CCHaR-2
20
Drome-TrissinR
Drome-SKR
1

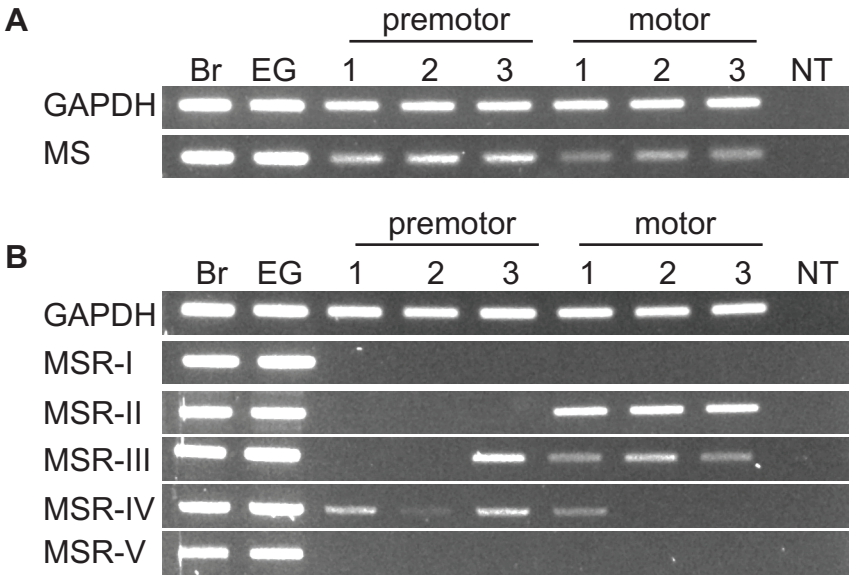
A
premotor
motor
Br
EG
1
2
3
1
2
3
NT
GAPDH
MS
B
premotor
motor
Br
EG
1
2
3
1
2
3
NT
GAPDH
MSR-I
MSR-II
MSR-III
MSR-IV
MSR-V